A FAST CODE ACQUISITION ALGORITHM FOR WCDMA UPLINK

A Thesis Submitted

In Partial Fulfillment of the Requirements

for the Degree of

Master in Technology

by

Snehamoy Banerjee

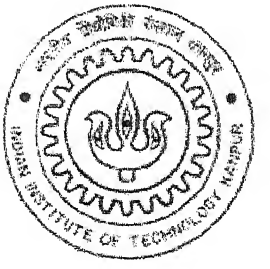

to the

DEPARTMENT OF ELECTRICAL ENGINEERING

INDIAN INSTITUTE OF TECHNOLOGY, KANPUR

August 2004

CERTIFICATE

It is certified that the work contained in the thesis entitled "**A Fast Code Acquisition Algorithm for WCDMA Uplink**", by **Snehamoy Banerjee**, has been carried out under my supervision and that this work has not been submitted elsewhere for a degree.

Dr Ajit Kumar Chaturvedi

Department of Electrical Engineering

Indian Institute of Technology

Kanpur – 208016

August, 2004

INDIAN INSTITUTTE OF TECHNOLOGY, KANPUR

Abstract/SYNOPSIS

Name of Student: Snehamoy Banerjee **Roll No.:** Y210432

Degree for which submitted: M.Tech **Department:** EE

Thesis Title: **"A fast code acquisition algorithm for WCDMA uplink"**

Name of thesis supervisor: Dr Ajit Kumar Chaturvedi

Month and year of thesis submission: August 2004

The existing 256 chips long complex scrambling code in WCDMA for high data rate users is not suitable for delay sensitive applications. A new fast code acquisition algorithm for WCDMA uplink is proposed. The complex part of the user specific short scrambling code is concatenated with length 13 binary Barker sequence at the 1st and 129th chip. A Barker Code Match Filter is used at the Base Station for joint detection of multipath signals of different Mobile Stations using Constant False Alarm Rate detection. For user specific code acquisition, a parallel search by Breadth-First Tree Search method using Truncated Sequential Probability Ratio test is used. The results obtained by simulation indicate that the mean acquisition time is much less than the full length searches.

Acknowledgments

I wish to whole heartedly thank my supervisor, Dr Ajit Kumar Chaturvedi, for his guidance and support throughout the duration of the research. I would also like to thank Prof. DSc. Christo Kabakchiev of the Institute of Information Technologies from the Bulgarian Academy of Sciences for his guidance in developing the analysis for CFAR detection system. I am also thankful to Prof James Ritcey of the University of Washington, Seattle for his suggestion of literature relating to the analysis of CFAR acquisition of PN sequence. Sincere thanks are also due to Prof Dilip Sarwate from the University of Illinois for suggesting literature relating to Parallel Code Acquisition systems.

I am also thankful to my colleagues who have been a source of inspiration and entertainment at hard times. I also sincerely thank my dear friend Appuswamy Rathinakumar for his valuable help and encouragement.

Finally, I thank my parents and brother who have stood the silence of long absence from home with prayers and good wishes for me.

Contents

List of Figures

Chapter 1

Introduction

1.1 Motivation

With the convergence of Computers and Communication systems there is a desire for greater bandwidth and more advanced systems while being wireless. The voice and data rates available in the first and second generation mobile communication systems no longer meet the growing demands in the twenty first century. High speed Internet and multimedia services are the order of the day. The third-generation (3G) mobile systems (called IMT-2000) are being designed to support wideband services, at data rates as high as 2 Mbps, with the same quality as a fixed network [1] [2] [3] [4]. Everyone desires that the wireless systems should be able to provide the same QoS guarantees as that of the wired systems. In order to realize this need, a new wideband wireless access technology incorporating recent technologies should be made possible.

Wideband direct sequence code division multiple access (WCDMA) is a predominant technology for wireless systems of the third generation. WCDMA is designed to offer flexible wideband services such as Internet access and real time QoS. However, these services are handicapped due to the physical limitations imposed by the wireless channel such as bandwidth constraints, multipath fading, noise, Doppler shift, multiple access interference etc. These pose a technical challenge in designing systems of high bandwidth for mobile communication applications [5] [6] [7] [1] [8] [9] .

To combat the effects of multipath fading, a Rake receiver is used to coherently combine the multipath components in WCDMA systems. Theoretically, it may be possible to combine a

large number of paths under no restriction of resources. This, however, is not feasible under most practical situations due to prohibitive complexity. In addition, certain real time applications are delay sensitive and demand that the processing time taken be as low as possible. Hence, designing a low complexity receiver with minimum processing time is an open problem.

1.2 Previous Work

In the past few decades extensive research work has been carried out in the field of code acquisition and various methods have been suggested by a number of them. Most of the researchers have considered AWGN channel model with Multiple Access Interference (MAI) and Inter Path Interference (IPI) modelled as white/coloured noise. However in advanced receivers the MAI and IPI are considered as structured and the correlation is taken into account. Limited work has been done in this field.

In the case of parallel schemes, Rick and Milstein [10] present a parallel PN code acquisition scheme for the reverse link of a cellular CDMA system. Dong and Blostein [11] suggested a tree-search based searcher. The model of a terrestrial mobile communication channel incorporates the effect of MAI, shadowing, power control error, vehicle speed, voice activity and sectorisation. The result shows that the system user capacity based on acquisition performance criteria is less than the capacity based on BSR criteria for certain ranges of system parameters. The effects of data modulation on the performance of parallel code acquisition scheme are reported in [12].

In serial search method Deng [13] proposes a burst mode PN acquisition processor for non-coherent detection. This MF based PN code acquisition processor achieved a mean acquisition time of less than 10 bits over a range of chip – noise ratio (CNR) from 7 dB to 8 dB. Chang, Park and Lee [14] proposed a double dwell code acquisition system with a serial search that

operates simultaneously with verification in long-code CDMA. For the search block, a MF is used for fast acquisition. For the verification block, an active correlator is used to reduce the complexity. The performance enhancement of this scheme mainly lies in reducing the false alarm probability by adding the verification stage while maintaining short acquisition time.

Tree-Search detector has been studied as a low complexity approach in various research areas of wireless communication systems. In [15], a simple reduced tree search detection of the breadth-first type is applied to sub-optimal joint multiuser detection bit-synchronous CDMA systems over both Gaussian and two-path Rayleigh fading channel by Wei and Rasmussen. Xie and Rushforth combined sub-optimum tree search algorithm with a recursive least-squares estimators of complex signal amplitude for joint Maximum Likelihood (ML) sequence detection and parameter estimation [16]. In [17], tree structured signal detection in V-BLAST system is proposed. It is found in [15], that tree search detector achieves near-optimum performance at a very low complexity. Tree-search scheme in conjunction with sequential PN code acquisition to reduce prohibitive complexity of parallel PN code acquisition have been suggested by Dong and Blostein [11]. However, the emphasis of their work has been more towards reduction of complexity and performance of gain combining technique when tree search is employed. Moreover, the system had inherent problems of rejection of large number of paths if null-hypothesis decision takes place at initial stages of the search. The paper has not made an attempt in studying the performance of the detection technique and suggesting methods for memory reduction and performance enhancement. There are short-comings in the statistical model considered in their paper.

1.3 Summary of Contributions

The contributions of this thesis are:

- Propose a new parallel code acquisition scheme with two different phases of operation. First multipath detection followed by user detection within each multipath.

- Propose change in the existing WCDMA uplink pilot channel structure by concatenating the imaginary part of the complex scrambling code with Barker Sequence for joint detection of multipath signals of all uplink users.

- Use the Constant False Alarm Rate (CFAR) algorithm for joint detection of multipath signals of all uplink users with the help of Barker Sequence.

- Analyze and study the changes in autocorrelation and cross-correlation properties of the pilot signal as a consequence of the proposed change.

- Propose a Tree search method using sequential detection for users present in each multipath.

- Obtain analytical expression for the test statistics using Truncated Sequential Probability Ratio test being used in the Tree search.

- Study the channel estimation being carried out for each user in a multipath during Tree search.

- Analyze and study the mean acquisition time and average sample size for the TSPRT.

1.4 Thesis Outline

In the following chapters, we propose a new low-complexity receiver architecture for fast code acquisition in uplink WCDMA receiver in which path detection, user detection and channel estimation are also incorporated. The objective of this study is to achieve a low-complexity fast code acquisition in uplink WCDMA.

We begin our study with a brief introduction to WCDMA communication systems in Chapter 2. We will see the existing WCDMA uplink system in light of the advantages and disadvantages

of code acquisition. Following this we formulate the problem to be solved in this thesis work and the corresponding system environment.

In Chapter 3, we have a treatment on the Constant False Alarm Rate (CFAR) method of detection. The chapter has an analysis on CFAR detection for Rayleigh faded signals and another analysis for PN sequence acquisition using CFAR detection for signals at the output of a correlator. Beginning with a Fixed Sample Size (FSS) test, we shall be following it by a treatment on Truncated Sequential Hypothesis Test (TSPRT) and its advantages over FSS. We will conclude with a description on Multistage Hypothesis Test (MHT), which is a modified form of TSPRT.

Chapter 4 forms the core of the thesis work. We will suggest the changes required and see the resulting properties of the modified sequences. Next, the joint detection of multipaths by CFAR is covered. We then proceed further with an insight into partial correlation properties which will be instrumental for sequential detection.

In chapter 5 we have the results of computer simulation and performance analysis of proposed algorithm.

Chapter 6 summarizes the conclusion of this thesis and presents topics for future research.

Chapter 2

Background of WCDMA Uplink Receiver

2.1 Introduction

A spread spectrum CDMA scheme is one in which the transmitted signal is spread over a wide frequency band, much wider than the minimum bandwidth required to transmit the information which is being sent [9]. It employs a waveform that appears random to everyone other than the intended receiver of the transmitted waveform. For the convenience of generation and synchronization by the receiver, the waveform is pseudo-random, meaning that it can be generated by precise mathematical rules, but statistically it nearly satisfies the requirements of a truly random sequence.

A CDMA system has several advantages over the conventional narrowband TDMA or FDMA systems; such as one-cell frequency reuse, inherent resistance to multipath fading, narrowband interference rejection, soft capacity, soft hand-off, simplification of channel allocation problem, ability to exploit silent periods in speech voice activity, inherent message privacy and low probability of interception [18] [19] [20] [21] [22]. Though CDMA promises to be advantageous, there are many technical issues to be resolved. Synchronisation of PN sequences is difficult to achieve in the presence of multipath effects, Doppler shifts and fading. Fast power control is essential in the reverse link in order to overcome the near-far effects. Multiple Access Interference (MAI), Inter Path Interference (IPI) and thermal noise are the capacity limiting factors in CDMA. The situation in uplink is further aggravated due to the random offset between multipath signals of the same user and different users causing correlation between them. This emphasizes the requirement to design better sequences. This results in the MAI and IPI as not being Additive White Gaussian Noise (AWGN) but as a more structured

interference thereby making the requirement of advanced Multi-User Detection (MUD) techniques necessary. The advanced receivers provide better interference cancellation features resulting in better performance and network capacity improvement at the cost increased complexity of the receiver. Moreover, for packet data communication system, there is an additional requirement of fast code acquisition for real time Quality of Service (QoS) applications. Thus, there is a need to design a low complexity receiver architecture which is a trade-off between performance and complexity.

2.2 Technical Features of WCDMA

In WCDMA systems, there are several new requirements: high spectral efficiency, high data rate, inter-system handover and multimedia communications with different QoS of multiplexed voice, data, image and video as well as different delay requirements from delay sensitive real-time traffic to delay flexible packet data. To meet these varied requirement, more sophisticated signal processing and communication techniques are proposed [4] [23] [24] [3]. These techniques include: short complex scrambling codes concatenated by orthogonal variable-spreading factor (OVSF) channelisation codes [23] [1], time multiplexed pilot channel structure and I/Q code-multiplexed pilot channel structure [25], fast transmit power control (TPC) [1], pilot symbol aided (PSA) coherent delay lock loop (CDLL), PSA coherent code acquisition, coherent RAKE combining, fast cell search under asynchronous operation, soft and softer handover, inter-frequency handover, blind bit rate detection, transmit diversity, multiuser detection, turbo coding and smart antennas [26] [8].

2.2.1 Spreading Codes

The spreading codes in CDMA may be classified into short codes and long codes. A short spreading code has a period equal to the symbol duration and the long spreading codes have a period which is much longer than the symbol duration. In long code systems the correlation

between users changes from bit to bit and MAI is therefore random in time. This causes the performance for different users to be statistically identical. Short codes have cross-correlations that remain unchanged over time and at times cause performance degradations over longer period of time.

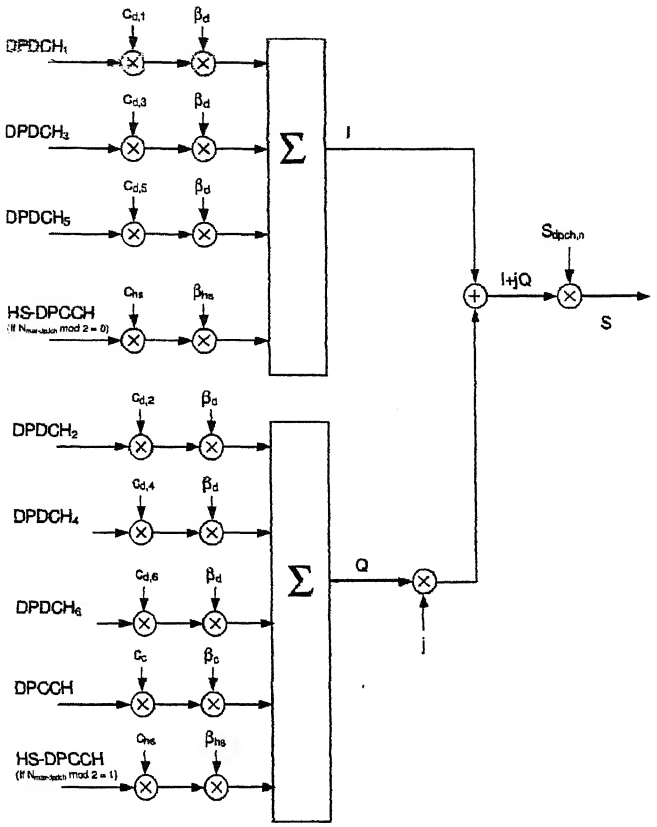

Figure 2.1: Spreading for uplink DPCCH, DPDCHs and HS-DPCCH

A WCDMA system uses a combination of short and long codes and hence has multiple spreading. The data is first spread by an OVSF code followed by spreading by a PN sequence. This second level spreading is cell-specific in the downlink but common to all users of that cell and it is user-specific in the uplink. The short orthogonal codes (OVSF) are called as channelisation codes and the PN codes are called as scrambling code. Each transmission from either a BS or a MS is distinguished by the combination of a channelisation code and scrambling code. The PN codes in WCDMA are of either long or short type. The spreading

for uplink WCDMA is shown in Figure 2.1 [27] and the channelisation code is shown in Figure 2.2.

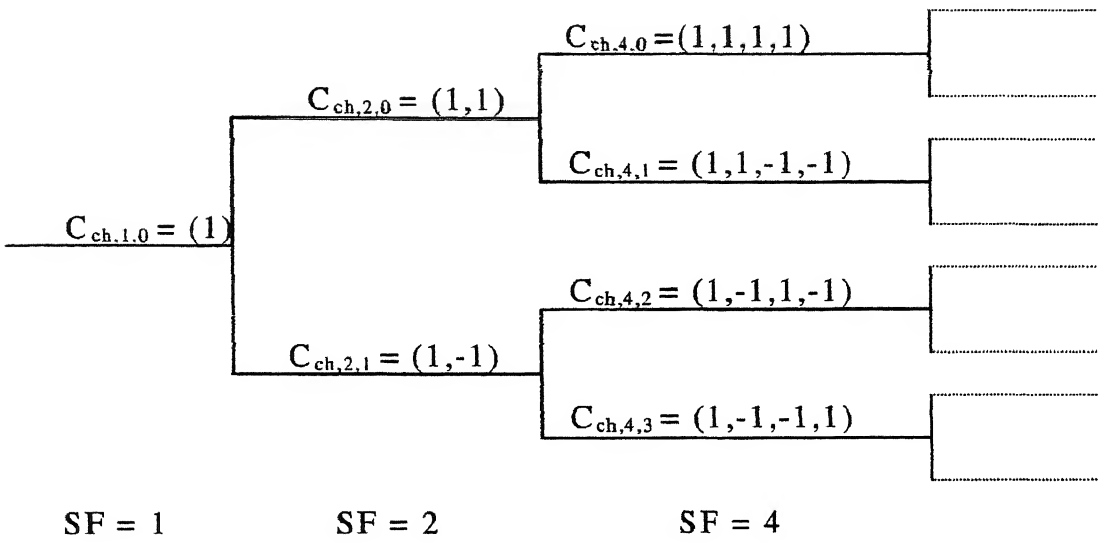

Figure 2.2: Code-tree for generation of Orthogonal Variable Spreading Factor (OVSF) codes

In Figure 2.2, the channelisation codes are uniquely described as $C_{ch,SF,k}$, where SF is the spreading factor of the code and k is the code number, $0 \leq k \leq SF-1$. Each level in the code tree defines channelisation codes of length SF, corresponding to a spreading factor of SF in Figure 2.2.

The generation method for the channelisation code is defined as:

$$C_{ch,1,0} = 1,$$

$$\begin{bmatrix} C_{ch,2,0} \\ C_{ch,2,1} \end{bmatrix} = \begin{bmatrix} C_{ch,1,0} & C_{ch,1,0} \\ C_{ch,1,0} & -C_{ch,1,0} \end{bmatrix} = \begin{bmatrix} 1 & 1 \\ 1 & -1 \end{bmatrix}$$

$$\begin{bmatrix} C_{ch,2^{(n+1)},0} \\ C_{ch,2^{(n+1)},1} \\ C_{ch,2^{(n+1)},2} \\ C_{ch,2^{(n+1)},3} \\ \vdots \\ C_{ch,2^{(n+1)},2^{(n+1)}-2} \\ C_{ch,2^{(n+1)},2^{(n+1)}-1} \end{bmatrix} = \begin{bmatrix} C_{ch,2^n,0} & C_{ch,2^n,0} \\ C_{ch,2^n,0} & -C_{ch,2^n,0} \\ C_{ch,2^n,1} & C_{ch,2^n,1} \\ C_{ch,2^n,1} & -C_{ch,2^n,1} \\ \vdots & \vdots \\ C_{ch,2^n,2^n-1} & C_{ch,2^n,2^n-1} \\ C_{ch,2^n,2^n-1} & -C_{ch,2^n,2^n-1} \end{bmatrix}$$

The leftmost value in each channelisation code word corresponds to the chip transmitted first in time.

2.2.2 Scrambling Codes

WCDMA uses two types of scrambling codes: the long codes and the short codes. The long scrambling sequences $c_{long,1,n}$ and $c_{long,2,n}$ are constructed from position wise modulo 2 sum of 38400 chip segments of two binary *m*-sequences generated by means of two generator polynomials of degree 25. Let *x*, and *y* be the two *m*-sequences respectively. The *x* sequence is constructed using the primitive (over GF(2)) polynomial $X^{25}+X^3+1$. The *y* sequence is constructed using the polynomial $X^{25}+X^3+X^2+X+1$. The resulting sequences thus constitute segments of a set of Gold sequences. The sequence $c_{long,2,n}$ is a 16777232 chip shifted version of the sequence $c_{long,1,n}$.

Since the primary concern of this thesis is relating to short scrambling codes for uplink WCDMA, we shall see in detail about this sequence. The short scrambling sequences $c_{short,1,n}(i)$ and $c_{short,2,n}(i)$ are defined from a sequence of the family of periodically extended S(2) codes.

Let $n_{23}n_{22}\ldots n_0$ be the 24 bit binary representation of the code number *n*.

The n^{th} quaternary S(2) sequence $z_n(i)$, $0 \le n \le 16777215$, is obtained by modulo 4 addition of three sequences, a quaternary sequence $a(i)$ and two binary sequences $b(i)$ and $d(i)$, where the initial loading of the three sequences is determined from the code number *n*. The sequence $z_n(i)$ of length 255 is generated according to the following relation:

- $z_n(i) = a(i) + 2b(i) + 2d(i)$ modulo 4, $i = 0, 1, \ldots, 254$;

where the quaternary sequence $a(i)$ is generated recursively by the polynomial $g_0(x) = x^8+x^5+3x^3+x^2+2x+1$ as:

- $a(0) = 2n_0 + 1$ modulo 4;
- $a(i) = 2n_i$ modulo 4, $i = 1, 2, \ldots, 7$;

- $a(i) = 3a(i\text{-}3) + a(i\text{-}5) + 3a(i\text{-}6) + 2a(i\text{-}7) + 3a(i\text{-}8)$ modulo 4, $i = 8, 9, \ldots, 254$;

and the binary sequence $b(i)$ is generated recursively by the polynomial $g_1(x) = x^8+x^7+x^5+x+1$ as

$b(i) = n_{8+i}$ modulo 2, $i = 0, 1, \ldots, 7$,

$b(i) = b(i\text{-}1) + b(i\text{-}3) + b(i\text{-}7) + b(i\text{-}8)$ modulo 2, $i = 8, 9, \ldots, 254$,

and the binary sequence $d(i)$ is generated recursively by the polynomial $g_2(x) = x^8+x^7+x^5+x^4+1$ as:

$d(i) = n_{16+i}$ modulo 2, $i = 0, 1, \ldots, 7$;

$d(i) = d(i\text{-}1) + d(i\text{-}3) + d(i\text{-}4) + d(i\text{-}8)$ modulo 2, $i = 8, 9, \ldots, 254$.

The sequence $z_n(i)$ is extended to length 256 chips by setting $z_n(255) = z_n(0)$.

The mapping from $z_n(i)$ to the real-valued binary sequences $c_{short,1,n}(i)$ and $c_{short,2,n}(i)$, , $i = 0, 1, \ldots, 255$ is defined in Table 2.1.

Finally, the complex-valued short scrambling sequence $C_{short,n}$ is defined as:

$$C_{short,n}(i) = c_{short,1,n}(i \bmod 256)\left(1 + j(-1)^i c_{short,2,n}(2\lfloor (i \bmod 256)/2 \rfloor)\right)$$

where $i = 0, 1, 2, \ldots$ and $\lfloor \rfloor$ denotes rounding to nearest lower integer.

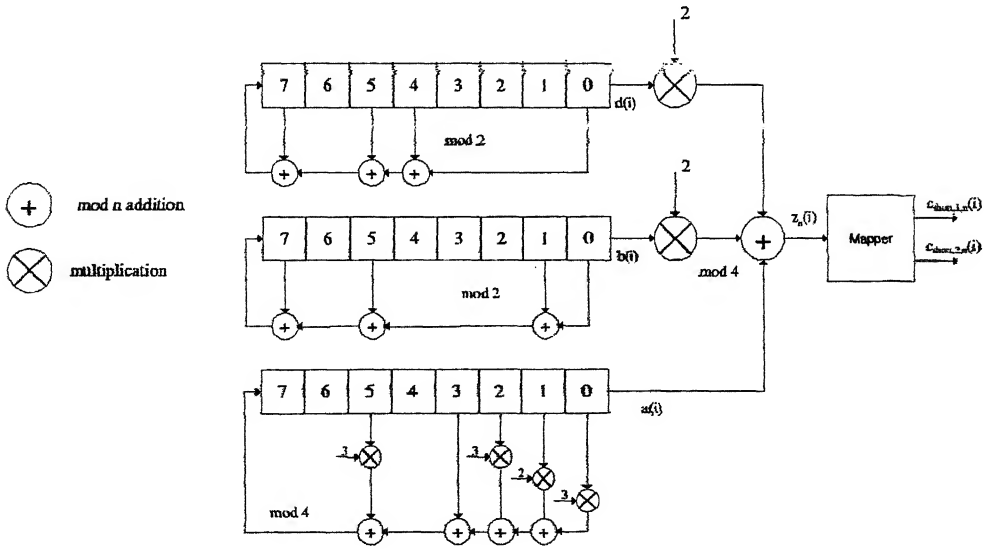

Figure 2.3: Uplink short scrambling sequence generator for 255 chip sequence

An implementation of the short scrambling sequence generator for the 255 chip sequence to be extended by one chip is shown in Figure 2.3

Table 2.1: Mapping from $z_n(i)$ to $c_{short,1,n}(i)$ and $c_{short,2,n}(i)$, $i = 0, 1, ..., 255$

$z_n(i)$	$c_{short,1,n}(i)$	$c_{short,2,n}(i)$
0	+1	+1
1	-1	+1
2	-1	-1
3	+1	-1

2.2.3 Pilot Channel Structure

The motivation for having a pilot channel is to have coherent RAKE combining, coherent code acquisition, channel tap weight estimation, power control and handoffs. There are two types of pilot channel in WCDMA system – common pilot channels and the dedicated pilot channels depending on whether the pilot symbols are shared by other users or not. According to the structure of pilot and data symbols, it is classified as time-multiplexed pilot channel and parallel pilot channel structure.

In parallel pilot channel structures, the pilot symbols are transmitted with the data symbols at the same time. The parallel transmission can be I/Q multiplexed, code multiplexing or frequency multiplexing. Pilot channel shown in Figure 2.4 provides good tracking of channel status more so in fading channels. But the spectral efficiency is low and the pilot channel will cause interference to other users even when no data communications occur. In time-multiplexed pilot channel structure as shown in Figure 2.5, the known N_{pi} pilot symbols are periodically multiplexed into N_D transmitted data symbols. Therefore, it is not suitable for delay sensitive real-time traffic such as voice and video transmission in circuit-switched systems. To allow for high speed data transmission over packet switched wireless networks, time- multiplexed pilot structure is favourable and it is proposed by Y Honda and M Mohar et al [28] [29]. The same shall be used in the thesis too.

Figure 2.4: Parallel pilot channel structure

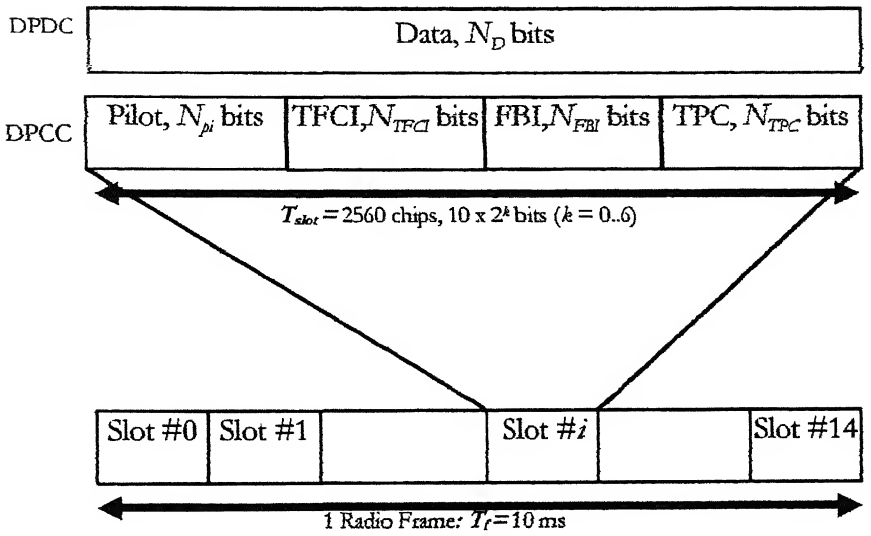

Figure 2.5 Time-multiplexed channel structure

2.3 WCDMA Receiver Architecture

2.3.1 Basics of RAKE Receiver

In WCDMA systems, the transmitted signal bandwidth is typically larger than the coherent bandwidth of the channel. The higher chip rates in WCDMA communication systems give more multipath diversity than that in narrowband CDMA. Conventional modulation schemes require an equalizer to undo the inter-symbol interference between adjacent symbols, CDMA spreading codes are designed to provide very low correlation between successive chips. If these multipath components are delayed in time by more than one chip duration, they appear like uncorrelated noise at a CDMA receiver and therefore equalizer is not needed. These uncorrelated paths are called resolvable paths because they could be separated by the correlation of a specific shift of the PN code [7].

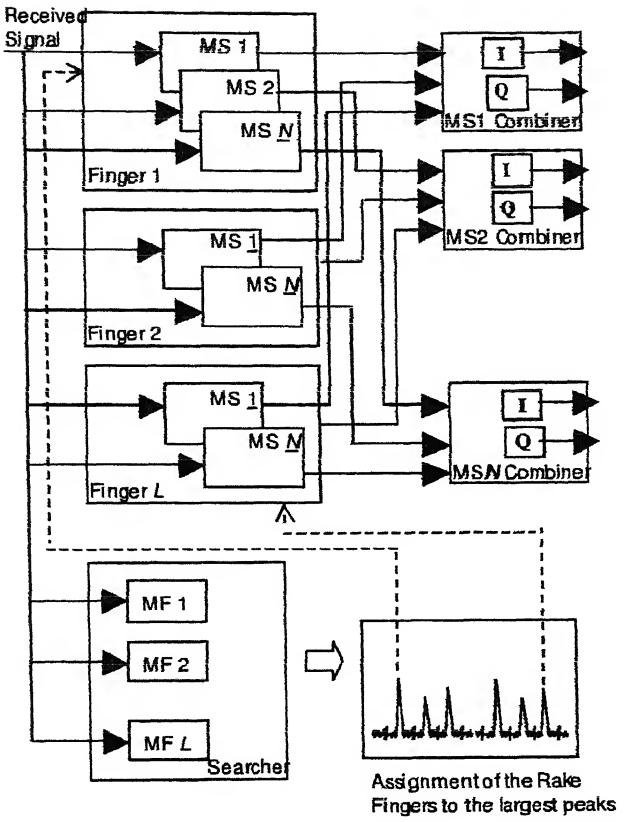

Figure 2.6: Uplink Rake Receiver for L path diversity

RAKE receiver attempts to collect the time–shifted replicas of the original signal by providing separate correlation for each resolvable path and the output of each correlator is weighted to provide a better estimate of the transmitted signal than is provided by a single component. Demodulation and bit decision are then based on the weighted output of a bank of correlators. The RAKE receiver is essentially a diversity receiver designed for CDMA where the diversity is provided by the fact that the multipath components are practically uncorrelated from one another when their relative propagation delays exceed by more than one chip duration [7]. In a RAKE receiver there are correlators each of which are matched to different paths with different delays. In the event of a path facing fading, the other paths being uncorrelated undergo relatively less fading and the RAKE receiver can correct the decision values. This would not have been possible had there been only one correlator. Decision is based on the combination of the separate decision statistics offered by the RAKE receiver. Thus, it provides

a form of diversity which can overcome fading and thereby improve CDMA reception. The RAKE receiver uses different forms of combination for the decision statistics namely Maximum Ratio Combining (MRC), Equal Gain Combining (EGC) and Generalized Gain Combining (GGC). In order to realize a high speed implementation of a RAKE receiver, correlators are replaced by Code Matched Filter (CMF). With increase in data rates there will be more and more multipaths implying that there will be a requirement of large number of CMF thereby increasing the complexity of the system. A typical RAKE receiver for an uplink in WCDMA is shown in Figure 2.6. The objective of the thesis is towards the design of a searcher for a RAKE receiver which continuously searches for changing multipaths and assigns fingers to the strongest multipaths.

2.3.2 Channel Estimation

Channel estimation problem in WCDMA receivers can be divided into two categories: multipath delay estimation and multipath tap amplitude and phase estimation. Theoretically, the channel estimation filter can be:

- a predictor: if it uses only the past samples to estimate the current channel coefficients
- a "filter": if it uses past and present samples for channel estimation
- a smoother: if it uses past, current and future samples

The removal of data modulation can be accomplished in data-aided (DA), decision directed (DD) or non data-aided (NDA) manner [6]. In DA mode, the receiver knows some of the transmitted symbols which are called pilot symbols. Based on the received signal and known pilot symbols, the receiver can estimate the channel profile. The DD channel estimators utilize the decisions of the receiver to remove the effect of data modulation, where there is a decision feedback at the output of quantizer. The NDA channel estimators (also called blind channel

estimators) estimates the channel without using data or decision. Instead, the statistical properties of the transmitted signals are exploited.

Channel tap weights estimation can be based on linear interpolation, low-order Gaussian interpolation [30] [31] and Wiener filtering [32]. However, the Wiener filter requires the knowledge of statistical properties of the fading channel, i.e., fading covariance matrix, which is difficult to estimate in practice though not impossible. Weighted Multi Slot Averaging (WMSA) is generally used for channel estimation filter that simply averages the pilot symbols belonging to more than two consecutive data slots.

2.3.2.1 Time-multiplexed Pilot Channel

In the time multiplexed pilot channel, there are N_p pilot symbols before N_D data symbols. Because fading remains almost constant over a period of N_p pilot symbols, the simple averaging of N_p consecutive pilot symbols improves the Signal to Noise and Interference Ratio (SNIR). The resultant channel estimate is given by:

$$\hat{w}(n) = \frac{1}{N_p} \sum_{m=0}^{N_p-1} r_l(m,n) \tag{2.1}$$

which approximates the instantaneous channel gain at the time position $n * T_{slot} + (N_p - 1) * T/2$ in the l^{th} slot of the l^{th} path, where $r_l(m,n)$ is the m^{th} received symbol at n^{th} data slot after RAKE combining. By averaging, the SNR of the channel estimate increases N_p times from the received SNR per symbol. As in the case of slow fading, the channel gain remains static over a period of several slots, we can coherently add several channel estimates by a linear filter with $2K$ taps to extend the observation interval. The channel gain varies slot-by-slot and hence the instantaneous channel estimates need to be weighted and summed. Therefore, the filter output is expressed as:

$$\hat{w}_l(n) = \sum_{i=0}^{K-1} \beta_{n,i} \hat{w}_l(n-i) + \sum_{i=0}^{K} \beta_{n,i-1} \hat{w}_l(n+i) \qquad (2.2)$$

where $\beta_{n,i}$ is the real-valued weighting factor and $2K$ is the observation interval represented by the number of slots. Using the weighting factors β's pre-stored in memory, the channel estimates $\hat{w}_l(n)$ are easily calculated from (2.1). In [25] the weighting factors optimised at the center of the slot are used for the reception of all the data symbols within the slot, that is $\beta_{n,i}$ is constant regardless of the symbol position of m.

$$\hat{w}_l(m,n) = \hat{w}_l(n) \quad m = N_{pi}, N_{pi}+1, \ldots\ldots\ldots\ldots, N_{pi}+N_D-1 \qquad (2.3)$$

By selecting the appropriate weighting factor β_i, accurate channel estimation is possible, particularly in slow fading environments, because a large number of pilot symbols belonging to multiple slots can be used. If the fading is slow, the $2K$ –tap WSMA channel estimation filter increases the SNR of the channel estimate by a factor of $N_P \left(\sum_{i=0}^{K-1} \beta_i\right)^2 \Big/ \sum_{i=0}^{K-1} \beta_i^2$. In the case of fast fading, the channel gain changes even within the slot. Consequently, we change the weight factors symbol-by-symbol within the slot to better track fast fading.

2.3.2.2 Parallel Pilot Channel

For parallel pilot channel, pilot symbols and data symbols are transmitted in different channels at the same time. We also weight and sum the continuously received pilot symbols and the weight coefficients are updated symbol-by-symbol. The filter output is given by:

$$\tilde{w}_l(m,n) = \frac{1}{2Z} \sum_{h=-Z+1}^{Z} \alpha_h \hat{w}(mT + nT_{slot} + hT) \qquad (2.4)$$

where α_h is the real-valued weighting factor and 2Z is the observation interval represented by the number of symbols.

The WMSA is a cascade of two filters: the first one is an integrator over a set of pilot symbols. It is followed by a linear filter with adaptive weights. Soft-decision statistics at the output of coherent RAKE combiner is represented at the m^{th} symbol of n^{th} slot associated with the l^{th} propagation path. $l = 0,1,\ldots\ldots\ldots, L-1$ as

$$\tilde{d}(n,m) = \sum_{l=0}^{L-1} r_l(m,n) * \tilde{w}_l(n) \qquad (2.5)$$

2.4 Problem Formulation

Radio propagation in the land mobile channel is characterized by multiple reflections, diffraction and attenuation of the signal energy. These are caused by natural obstacles/bodies such as hills, buildings, lamp posts etc resulting in multipath propagation. In the frequency selective multipath channel, the signal energy is smeared into a certain multipath delay profile, where multiple version of the transmitted signal are received with different amplitudes and times of arrival [7] [1].

In WCDMA systems, a wider bandwidth is allocated to support multimedia services and higher chip rates are used to multiplex the data streams of different users. An increased chip rate means reduced chip duration and path delay spreads over a larger number of chip periods. Therefore, more resolvable multipath is available at the receiver, where multipath components are spaced at least one chip period apart. At 3.84 Mcps, the waves travel 78 m in one chip duration $\left(3*10^8 m/3.84 Mcps\right)$. Besides, multipath channel profile is dynamically time-varying which requires a RAKE receiver with a variable number of RAKE fingers adapting to the time-varying channel state information (CSI).

An optimal RAKE receiver, known as Full Search RAKE receiver, requires unlimited resources (CMFs or correlators) so as to combine all of the possible multipath components [33]. Optimal performance is practically difficult to achieve because of prohibitive complexity and imperfect channel estimates. In the chapters to follow, we propose a new low complexity algorithm which causes a trade-off between optimality and complexity. The new algorithm is proposed for a WCDMA uplink receiver where we use a two-level detector. In the first stage the different multipaths of all users are detected and in the second stage detector the different users present in each multipath are detected and simultaneously channel estimation is done.

2.5 System Model in Thesis

In this thesis we consider an uplink WCDMA communication system working with Frequency Division Duplex (FDD). There are K active users in the system. Each user is presumed to have a maximum of L multipaths that may be combined in the RAKE receiver for multipath diversity.

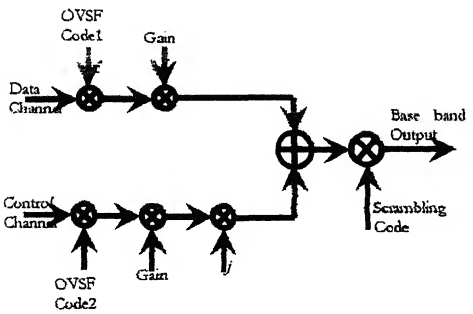

Figure 2.7: Uplink WCDMA transmitter model

The transmitter is simplified with one Dedicated Physical Data Channel (DPDCH) and one Dedicated Physical Control Channel (DPCCH) with I/Q multiplexing. The simplified system is shown in Figure 2.7. Further since our thesis relates to code acquisition in the RAKE receiver searcher, we shall deal only with the base-band signal processing for DPCCH.

The following assumptions have been made:

- Binary phase shift keying (BPSK) modulation is used at the transmitter with rectangular chip pulse shape.
- Extended Gold code family with length of 256 PN chips is used as the short scrambling codes.
- Coherent detection is used, aided by a separate pilot channel.
- The multiple signal paths of each user are resolvable. An exponentially decaying multipath intensity profile (MIP) is used.
- Synchronous CDMA is achieved where the dominant paths of each user are synchronized in terms of symbol boundary.
- Fractional portion of PN chip offsets of multipath propagation are ignored.
- Fast transmit power control of the dominant path is used to compensate the path loss, shadowing and fast fading so that the near-far problem is avoided.
- The number of resolvable multipaths is unknown at the receiver.
- An isolated cell is considered with one base station in the center and K active users, therefore, no inter-cell interference exists.
- Rayleigh fading channel with Additive White Gaussian Noise AWGN. The channel noise is modeled as AWGN.

2.6 Uplink Signal and Channel Model

The model for the thesis and assumptions has been discussed in section 2.5. However, for simplicity, only the DPCCH with binary phase shift keying (BPSK) modulation and square pulse shape are assumed. The following WCDMA system uses baseband discrete-time signal and system model.

2.6.1 WCDMA Transmitter

The transmitter uses direct sequence spread spectrum (DSSS) modulation. The information data symbols are spread by user specified short spreading PN code with symbol length and BPSK modulated. Finally, it is transmitted on a radio carrier. The transmitted digital spread spectrum signal from user i in one symbol interval can be represented by:

$$s_i(n) = \hat{c}_n^{(i)} d_i \tag{2.6}$$

where the chip time index n = 1, ...G and G is the number of chips per symbol or processing gain. $\hat{c}_n^{(i)}$ is the chip value of PN code of user i at time index n, $\hat{c}_n^{(i)} \in \{-1,1\}$, d_i is the transmitted symbol value at this symbol interval. The transmitted signal will be dispersive by the channel and it is subject to interference and AWGN.

2.6.2 The Multipath Channel Model

Frequency selective Rayleigh Fading is used to model the reverse channel from the mobile terminal to the base station. The multipath radio channel for i^{th} mobile may be described as a wideband tapped delay line (WTDL) model with statistically independent time-variant tap weight β_{ij}:

$$h_i(n) = \sum_{j=1}^{L} \beta_{ij} \delta(n - \tau_{ij}) \tag{2.7}$$

where L is the total number of multipaths, which is dynamic because of the time-varying characteristic of wideband wireless channels [6]. The index j represents one of L multipaths experienced by the i^{th} user and τ_{ij} is the relative integer chip time delay with respect to the first arriving component for j^{th} path of i^{th} user.

2.6.3 WCDMA Receiver

In the multipoint-to-point uplink CDMA channel, the received WCDMA signal is superposition of K channel outputs from K active users, corrupted by channel noise:

$$r(n) = \sum_{i=1}^{K} s_i(n) * h_i(n) + z(n) \tag{2.8}$$

where symbol * indicates convolution and $z(n)$ is AWGN with a double sided power spectral density of $\frac{N_0}{2}$. K is the total number of users. Hence, after RF analog downconversion, chip pulse shaping filtering and chip-rate sampling, the equivalent received baseband discrete-time signal in one symbol period is obtained by inserting (2.7) into (2.8) yielding:

$$r(n) = \sum_{i=1}^{K} \sum_{j=1}^{L} \beta_{ij} d_i \hat{c}^{(i)}_{n-\tau_{ij}} + z(n) \tag{2.9}$$

where $\hat{c}^{(i)}_{n-\tau_{ij}}$ is the PN code of user i after a τ_{ij} circular shift. Since code acquisition is aided by pilot symbols which are not data modulated, $d_i = 1$.

2.7 Code Acquisition of Multipath Signals

In WCDMA system, code acquisition is very important because reception of WCDMA signals is possible only after the receiver is able to synchronise the local PN code with the PN code in the transmission intended for it [34]. The other channel parameters may be estimated only

when the acquisition has taken place. Code acquisition is generally carried out in two steps: acquisition and tracking. Code acquisition is the process by which the receiver attempts to align its local PN code's phase to the incoming signal within half or less than half of a-chip duration. Since the autocorrelation peak is much greater than the side lobes, a correlation between the local PN code and the received signal yields are estimate of whether the sequences are aligned.

Many different types of PN code acquisition architectures exist, the most commonly used architectures are the active synchronous correlators and passive matched filter implementation [13]. For synchronous correlator implementation, each new offset value must be computed with integration over the symbol period T_s, which results in longer acquisition time. For passive matched filter implementation, a code filter matched to the PN code sequence is used. The despread signal components appear sequentially at the matched filter output, the passive matched filter can do the code correlations for different offsets much faster than the serial correlator even though output values are mathematically equivalent [35]. The disadvantage of matched filter is its high complexity.

At the searcher in the RAKE receiver, the locally generated code sequence will be phase matched with that of the received signal. Code acquisition is the process of determining the time delay of each path of each user. Strictly speaking, determining the exact sampling time is an estimation problem. In order to reduce the problem to one of finite dimensionality, the delay is assumed to be a multiple of chip-time T_c. In other words, chip-synchronous environment is assumed.

2.7.1 Conventional Matched Filter Approach

In a conventional MF receiver, the received signal filtered by a pre-determined Code Matched Filter (CMF), where each possible delay of the PN sequence of the desired user is encoded as a

separate set of co-efficient. The received signal is match filtered by the PN sequence for the i^{th} user with integer time delay τ_{ij} of the j^{th} path and is denoted by Z_{ij}.

In section 2.2.2 we have given a description on the generation of short spreading sequences or the complex scrambling codes of length 256 in WCDMA. These imaginary part of the sequences are used for code acquisition and channel estimation.

Let us consider the imaginary part of the complex sequence and represent it as $\{c_n^{(i)}\}$, where $i = 0,1,\ldots,M-1$ and $n = 0,1,2,\ldots,G-1$. Here M is the number of sequences in the family (M = 16777215) and G is the period of the sequence (G = 256). For a conventional MF case, we have at the output of the CMF matched to user i with delay of j chips in a system with K users and each having L multipath where L is a random variable:

$$\begin{aligned} Z_{ij} &= \sum_{n=1}^{G} r(n)\hat{c}_{n-\tau_{ij}}^{(i)} \\ &= \beta_{ij}G + \sum_{n=1}^{G}\sum_{k=1}^{K}\sum_{\substack{l=1 \\ k,l\neq i,j}}^{L}(\beta_{kl}d_k\hat{c}_{n-\tau_{kl}}^{(k)} + z(n))\hat{c}_{n-\tau_{ij}}^{(i)} \\ &= \beta_{ij}G + IN_{ij} \end{aligned} \tag{2.10}$$

where (2.9) is used and where

$$IN_{ij} = \sum_{n=1}^{G}\sum_{k=1}^{K}\sum_{\substack{l=1 \\ k,l\neq i,j}}^{L}(\beta_{kl}d_k\hat{c}_{n-\tau_{kl}}^{(k)} + z(n))\hat{c}_{n-\tau_{ij}}^{(i)} \tag{2.11}$$

The signal from the i^{th} mobile with shift τ_{ij} will have a processing gain of G chips per bit, and the interference from other users can be modelled as AWGN type interference [6]. The correlation statistics Z_{ij} can be used to test the presence of the signal delayed by jT_c seconds from the i^{th} mobile. In (2.11) the first term results in a combination of MAI (if $k \neq i$), IPI (if $k = i$ and $l \neq j$) and the second term results in thermal noise.

Chapter 3

Detection Techniques for Code Acquisition

3.1 Introduction

Signal detection problems in wireless communications receiver design are generally M-ary hypothesis testing. There we wish to decide among M possible statistical situations describing the observations. For any given detection problems, there are a number of possible decision strategies or rules that can be applied. However we will choose a decision strategy that is optimum in some way for our algorithm. We shall employ two different strategies for the proposed algorithm. First, a Constant False Alarm Rate (CFAR) detection scheme is employed for detection of all possible existing multipaths. Second sequential detection scheme using TSPRT is used for user specific code acquisition within each detected multipath.

3.2 Constant False Alarm Rate Detection

There are two aspects of CFAR detection. First, we analyse the CFAR detection scheme for a Rayleigh faded signal. Second, the PN sequence acquisition using CFAR detection using a CMF.

3.2.1 Conventional CFAR Detection

The basic concept of a CFAR technique is that the voltage of a test cell is compared to that of a set of reference cells. If the test cell voltage is "similar" to those of the reference cells, a signal-absent decision is made. If the test cell voltage is not similar, a signal-present decision is made. CFAR processor using range window for reference cells is shown in Figure 3.1.

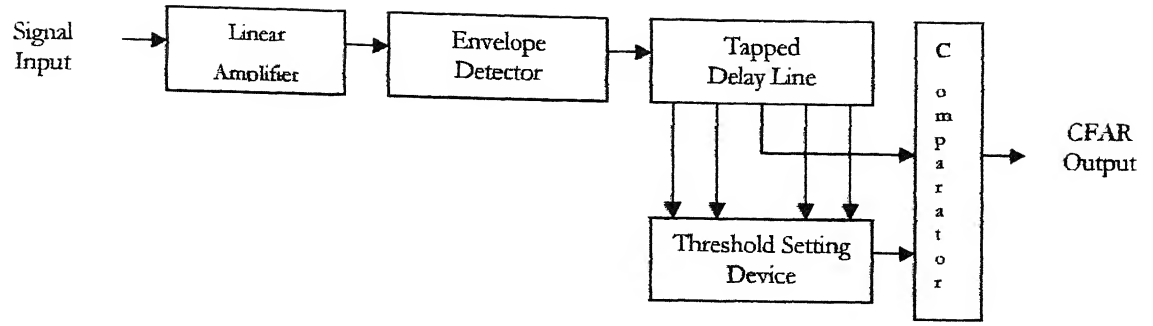

Figure 3.1: CFAR Processor

3.2.1.1 Methods for Obtaining a Set of Reference Cells

There are several methods of obtaining a set of reference cells [36]. The proper method depends on the type of interference environment. One common technique, shown in Figure 3.1, uses a range interval bracketing the test cell as the reference cells. Use of this set implies that the characteristics of the interference do not change over the range interval of the reference and test cells. This assumption is true when the interference environment consists of the sum of thermal noise and constant-power jamming noise. The assumption is not true for environments that include ground clutter as the clutter cross section tends to change significantly in relatively small range increments.

3.2.1.2 Detection Threshold of CFAR Processor

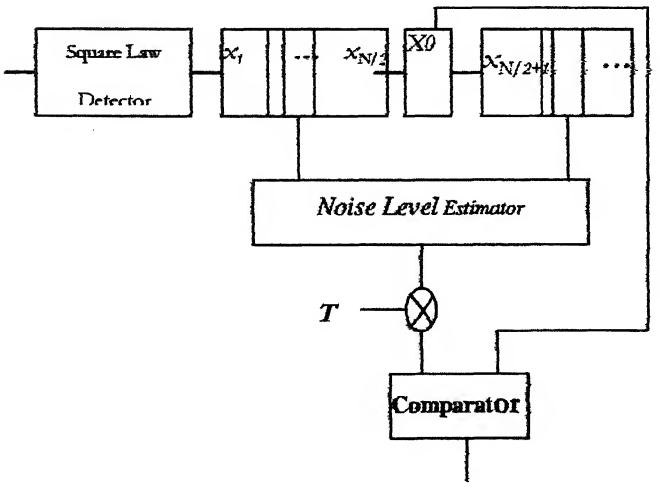

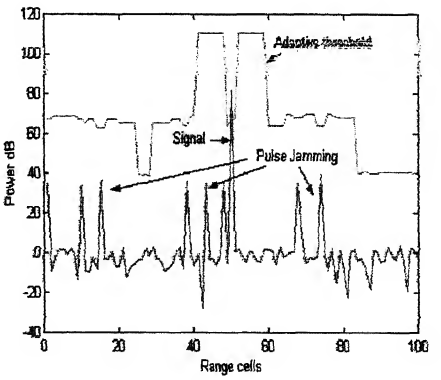

Figure 3.2: Block diagram of the CFAR processor **Figure 3.3: Signal detection**

The received signal $x(t)$ is square law detected and sampled in range by the $N+1$ range resolution cells as shown in Figure 3.2. The set of samples $(x)_N$ is processed resulting in a noise level estimate V. The estimate V is multiplied by a predetermined scale factor T resulting in a pulse detection threshold H_D.

3.2.1.3 Pulse Detection in CA CFAR Processor

The sample from the test resolution cell x_0 is compared with the threshold H_D. The multipath signal detection is declared if the sample x_0 exceeds the threshold H_D (Fig. 3.2).

$$H_D = VT \tag{3.1}$$

where T is the scale factor, maintained constant the false alarm probability, V is the estimate of the noise level in the cell under test

$$V = \sum_{i=1}^{N} x_i \tag{3.2}$$

where N is the number of reference cells. The output of the cell under test is compared to the adaptive threshold according to

$$\begin{cases} H_1 \text{ (multipath signal is present)}: & \text{if} \quad x_0 \geq H_D \\ H_0 \text{ (multipath signal absent)}: & \text{if} \quad x_0 < H_D \end{cases} \tag{3.3}$$

where H_1 and H_0 are hypothesis that the presence or the absence of a target in the test cell.

3.2.1.4 Fluctuating Signal

Essentially most outdoor mobile communication signals produce amplitudes that are Rayleigh distributed (exponential distribution of power, or cross section) [37] [38]. In general, the effect of fluctuation requires higher signal-to-noise ratios for high probability of detection and lower

values for low probability of detection than those required with no fluctuating signal. Swerling [39, 40] has considered four cases, which differ in the assumed rate of fluctuation and the assumed statistical distribution of the cross section. The two assumed rate are:

- a relatively slow fluctuation of the signal, such that the values of λ_0 for successive chips of a multipath are statistically independent but remain virtually constant from one pulse to the next, and

- a relatively fast fluctuation, such that the values of λ_0 are independent from pulse to pulse within one symbol duration (i.e., during the integration time). The first of the two assumed distribution for the received-signal voltage is of the Rayleigh form (3.4), which means that the mean amplitude of the signal λ_0 has a probability density function given by

$$f(x|H_i)=\begin{cases}\dfrac{1}{\lambda_0(1+s)}\exp\left(\dfrac{-x}{\lambda_0(1+s)}\right) & H_1\\ \dfrac{1}{\lambda_0}\exp\left(\dfrac{-x}{\lambda_0}\right) & H_0\end{cases} \tag{3.4}$$

where λ_0 is the average amplitude over all signal fluctuation, s is the signal-to-noise ratio. The second assumed cross-section density function is

$$f(x|H_i)=\begin{cases}\dfrac{4x}{(\lambda_0(1+s))^2}\exp\left(\dfrac{-2x}{\lambda_0(1+s)}\right) & H_1\\ \dfrac{4x}{\lambda_0}\exp\left(\dfrac{-2x}{\lambda_0}\right) & H_0\end{cases} \tag{3.5}$$

The first distribution (3.4) is observed when the received signal consists of many independent scattering elements of which no single one few predominate. Many mobile communication systems have approximately this characteristic at microwave frequencies, and seen largely in

complicated scattering environment, which are usually of this nature (NLOS). The second distribution (3.5) corresponds to that of a path having one main scattering element that predominates together with many smaller independent scattering elements (LOS with scattering). In summary, the cases considered are as follows:

- Case 1 Eq. (3.4), slow fluctuation. The chips received from the transmitter on any one symbol duration are of constant amplitude throughout the symbol duration, but uncorrelated from one symbol to another.

- Case 2 Eq. (3.4), fast fluctuation. The pdf is as for Case 1, but fluctuations are taken to be independent from chip to chip.

- Case 3 Eq. (3.5), slow fluctuation. The fluctuations are independent from scan to scan, but the pdf is given by (3.5).

- Case 4 Eq. (3.5), fast fluctuation. The pdf is as for Case 3, but fluctuations are independent from chip to chip.

- Case 5 Non fluctuating.

The pdf for cases 1 and 2 is indicative of a signal with many scatters of equal amplitude. These are typical for complicated multipaths like in dense urban areas. The pdf for cases 3 and 4 is indicative of a signal with one large scattered and many small scatters.

3.2.1.5 Analysis of the CA CFAR Detector

According to rule (3.3) the probability of pulse detection P_D may be found as [41] [42]

$$P_D = P(x_0 > TV|H_1) = \int_0^\infty f_V(V)dV \int_{TV}^\infty f(x_0/H_1)dx_0 \qquad (3.6)$$

where $f_V(V)$ is the pdf of the estimate V, and $f(x_0/H_1)$ is the conditional pdf of the test sample under hypothesis H_1.

The probability of false alarm is evaluated substituting $s = 0$ into expression (3.6).

$$P_{FA} = P(x_0 > TV|H_0) = \int_0^\infty f_V(V)dV \int_{TV}^\infty f(x_0/H_0)dx_0 \tag{3.7}$$

In other words, the probability of false alarm is determined in general by [43]

$$P_{FA} = E_V\{P(x_0 > TV|H_0)\} \tag{3.8}$$

which can also be written as

$$P_{FA} = E_V\left\{\int_{TV}^\infty \frac{1}{\lambda_0}\exp\left(\frac{-x_0}{\lambda_0}\right)dx_0\right\} = E_V\left\{\exp\left(\frac{-TV}{\lambda_0}\right)\right\} = M_V\left(\frac{T}{\lambda_0}\right) \tag{3.9}$$

where $M_V(.)$ denotes the moment generating function (MGF) of the random variable V. Similarly, the detection probability P_D is given by

$$P_D = E_V\{P(x_0 > TV|H_1)\} \tag{3.10}$$

Since under the signal-present hypothesis H_1 the mean $\lambda_0 = \lambda_0(1+s)$, we can determine P_D by simply replacing λ_0 with $\lambda_0(1+s)$ in (3.7).

$$P_D = M_V\left(\frac{T}{\lambda_0(1+s)}\right) \tag{3.11}$$

In conventional CA CFAR processor the noise level estimation V is formed as a sum of all outputs of the reference window. In this case the MGF of the estimate V is defined to be [41]:

$$M_V(U) = M_x^N(U) \tag{3.12}$$

where $M_x(U)$ is the MGF of the random variable x_i. The moment generation function may be found as Laplace transformation of the pdf $f(x)$

$$M_x(U) = \int_0^\infty \exp(-Ux) f(x) dx \tag{3.13}$$

The moment generation function of the random variable x_i is:

$$M_X(U) = \frac{1}{1+U\lambda_0} \tag{3.14}$$

The MGF of the estimate V (3.12) of CA CFAR detector is:

$$M_V(U) = \frac{1}{(1+\lambda_0 U)^N} \tag{3.15}$$

Assuming that the primary target in the test cell is fluctuating according to Swerling II model [39, 40], substituting (3.11) into equation (3.15) the probability of target signal detection is

$$P_D = \left[1 + \frac{T}{1+s}\right]^{-N} \tag{3.16}$$

Setting s=0, in equation (3.16), the design expression for the probability of false alarm is

$$P_{FA} = [1+T]^{-N} \tag{3.17}$$

The scaling factor T is then computed from equation (3.17) thus,

$$T = (P_{FA})^{-1/N} - 1 \tag{3.18}$$

As the number of reference range cells becomes large $(N \to \infty)$, the probability of detection approaches

$$P_D = \lim_{N\to\infty}\left[1+\frac{T}{1+s}\right]^{-N} = \exp\left(-\frac{T}{1+s}\right) \tag{3.19}$$

and the probability of false alarm approaches

$$P_{FA} = \lim_{N\to\infty}[1+T]^{-N} = \exp(-T) \tag{3.20}$$

Equations (3.19) and (3.20) are the expressions which describe the performance of the ideal (fixed threshold) detector. Thus, for homogeneous clutter background environment, the CA CFAR detector is the optimum detector in the sense that its probability of detection approaches that of the ideal fixed threshold detector, as the number of reference noise samples becomes very large.

The CA CFAR detector achieves the design probability of false alarm and a high detection probability in a homogeneous background environment, that is, when the received noise samples are identically distributed and statistically independent. In a real environment however the noise samples may not be homogeneous.

3.2.2 CFAR Acquisition of PN Sequence

In this section we analyse the CFAR detection scheme applied to the pdf of the output of a CMF. An introductory analysis to CFAR has been given in [9] and in the above section where we have found the threshold for CFAR for a signal in multipath Rayleigh fading channel. Further detailed analysis has been given in [44]. The I-Q Non-coherent CMF and the Threshold Setting block for one particular phase can be given as under. In this section we shall apply the threshold of CFAR in PN sequence acquisition.

The decision variable is square of a Gaussian Random Variable. It has a non-central χ^2 distribution at the stage H_1 and central χ^2 distribution at the stage H_0.

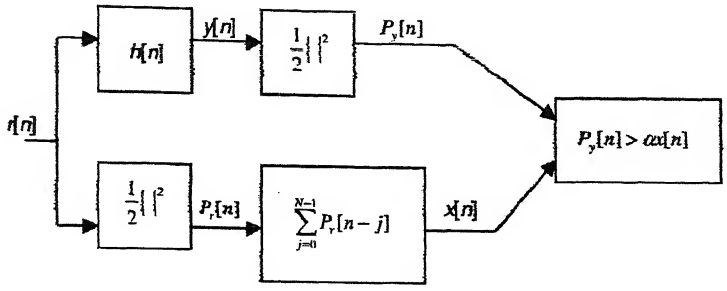

Figure 3.4: CFAR Adaptive Threshold Detector

To evaluate the probabilistic performance of a detector we need to model the output of the comparison filter at single sample time. Consider the received signal vector **r** to be a *Nx1* complex vector which corresponds to the last N samples of the received signal. Then accordingly

$$\mathbf{r}^t = [r[n], r[n-1], ..., r[n-(N-1)]] \tag{3.21}$$

Let the filter vector, **h**, be the *Nx1* complex vector containing the filter in correlation form as

$$\mathbf{h}^t = [h[0], h[1], ..., h[N-1]] \tag{3.22}$$

The output of the filter at a single point in time is the inner product of the received signal vector and the filter vector $\mathbf{y} = \mathbf{h}^\dagger \mathbf{x}$, where † represents the operation of conjugate transpose. The filter vector is normalized to have unit energy $|h|^2 = 1$, and can be one of N different filters of the system,

$$\mathbf{H} = \{\mathbf{h}_1, \mathbf{h}_2, ..., \mathbf{h}_N\}. \tag{3.23}$$

We model the received signal as the combination of a signal component and AWGN,

$$\mathbf{r} = A\mathbf{s} + \mathbf{w} \tag{3.24}$$

where **s** and **w** are *(Nx1)* complex column vectors. These are the signal vector (pilot with data value of 1) and AWGN vectors respectively. The noise vector is complex multivariate GWN with zero mean and correlation matrix $\frac{1}{2}E\{\mathbf{w}\mathbf{w}^{\dagger}\} = \sigma^2\mathbf{I}$. A is a real scalar amplitude that is related to the SNR of the signal. The SNR of the received code is defined with respect to the peak response of a CMF, $SNR = A^2/2\sigma^2$. For the peak response the signal vector, **s**, contains the code of the desired multipath (assuming that the pilot signal is unmodulated i.e.; with a value of 1)

$$\mathbf{s} = \mathbf{b} = [b[0], b[1], ..., b[N-1]] \text{ with } |b|^2 = 1$$

Since the code vector, **b**, has unit energy the signal vector **s** has variable energy between 0 and 1. The inner product of the signal vector, **s**, and the filter, **h**, define a location in a correlation function. The absolute value of the inner product can be defined as the correlation coefficient of the filter and the signal vector, $\rho = |\mathbf{h}^{\dagger}\mathbf{s}| = |\rho R + ji\rho|$. The first part is the desired signal part and the next part is a combination of IPI and MAI. If *i=j*, then it is IPI, i.e.; autocorrelation function and if $i \neq j$, then it is cross-correlation between the pilot signal and other modulated data resulting in MAI.

The constant false alarm rate is obtained by estimating the energy in the received signal and using this to adjust the threshold. Consider the case when no noise is present in the system. If we look at the ratio of $P_y[n]$ over $x[n]$ we obtain the CFAR normalized correlation function. Comparing a location in this function to the fixed threshold parameter T, is equivalent to

comparing $P_y[n]$ to the adaptive threshold $Tr[n]$. The ratio of $P_y[n]/r[n]$ will always be between 0 and 1, regardless of the amplitude of A. Defining each value in these correlation functions as a CFAR correlation coefficient, ρ_j. Where ρ_j is defined as

$$\rho_j = \frac{\rho^2}{1-\frac{|j|}{N}} \quad \text{and } j \text{ is the offset from the peak response.} \tag{3.25}$$

The aim is that at high SNR/no noise, the threshold should be so chosen that the peak response of the ACF will be detected while the range side lobes and cross-correlation values will not. As the energy in the noise increases a noise cloud forms around each point in the correlation function. At low SNR, the uncertainty each location in the ACF becomes large. This will give locations whose ρ_j is less than a, a positive probability being detection, $P_f > 0$. Also this will decrease the probability of detecting the peak response, $P_d < 1$. We would wish to set α for a given P_f and then evaluate P_d for varying SNR. The determination of P_f and P_d, consists of evaluating the probability of one random variable exceeding another. In the case of CFAR detector this is the probability that $P_y[n] > Tx[n]$. In the general case this is expressed as:

$$P = P_r\left[\frac{1}{2}\left|\mathbf{h}^\dagger\mathbf{r}\right|^2 > \alpha\frac{1}{2}\left|\mathbf{r}^\dagger\mathbf{r}\right|\right] \tag{3.26}$$

It is difficult to compute P because the LHS and RHS of the inequality are dependent (x). In order to overcome it, we will carryout a transformation into a new co-ordinate system that will allow for separation of the problem into sums of independent random variables. The new co-ordinate system should include **h** as one of its member. The basis can be represented as matrix

$\Phi = [\phi_0, \phi_1, ..., \phi_{N-1}]$ with $\phi_0 = \mathbf{h}$. Since the columns of Φ form a basis the matrix is unitary, $\Phi^\dagger \Phi = \mathbf{I}$.

The received signal can be represented as the linear combination of the basis set, $\mathbf{r} = \Phi\mathbf{a}$, where $\mathbf{a}$ is the (Nx1) column vector containing the coefficients of the basis vectors. The coefficients are obtained by projecting the received signal vector onto the basis set, $\mathbf{a} = \Phi^\dagger \mathbf{r}$. The coefficients are independent Gaussian random variables with (in new co-ordinate system) mean = $A\Phi^\dagger \mathbf{s}$ and variance = $\sigma^2 \mathbf{I}$.

Substituting for r in the LHS of the detection event procedures,

$$\frac{1}{2}\left|\mathbf{h}^\dagger \mathbf{r}\right|^2 = \frac{1}{2}\left|\mathbf{h}^\dagger \Phi \mathbf{a}\right|^2 = \frac{1}{2}\left|a_0\right|^2 \tag{3.27}$$

Doing the same for the RHS of the detection event gives,

$$\frac{1}{2}\left|\mathbf{r}^\dagger \mathbf{r}\right| = \frac{1}{2}(\Phi^\dagger \mathbf{a})^\dagger (\Phi^\dagger \mathbf{a}) = \frac{1}{2}\mathbf{a}^\dagger \mathbf{a} \tag{3.28}$$

When these representation are incorporated into the overall detection event the following simplification arises,

$$\left\{\frac{1}{2}\left|\mathbf{h}^\dagger \mathbf{r}\right|^2 > T\frac{1}{2}\left|\mathbf{r}^\dagger \mathbf{r}\right|\right\} \Rightarrow \left\{\frac{1}{2}\left|a_0\right|^2 > t\sum_{j=1}^{N-1}\left|a_j\right|^2\right\} \text{ where } t = T/(1-T) \tag{3.29}$$

The probability performance measures, *P*, now is the comparison of two independent random variables,

$$P = P_r\left[\frac{1}{2}\left|a_0\right|^2 > t\sum_{j=1}^{N-1}\frac{1}{2}\left|a_j\right|^2\right] \tag{3.30}$$

Define the random variable $v_j = \frac{1}{2}|a_j|^2$ with $j = 0,...,N-1$. Since the a_j`s are independent Gaussian random variables the $v_j$`s are independent non-central Chi-Squared random variables with two degrees of freedom. The Moment Generating Functions (MGF) of the v_j`s is given by,

$$h_{vj}(u) = E\{e^{-uv_j}\} = \frac{1}{(1+\sigma^2 u)} \exp\left\{ \frac{-\frac{1}{2}|A\phi_j^{\dagger}\mathbf{s}|^2 u}{1+\sigma^2 u} \right\} \tag{3.31}$$

Expressing the LHS and RHS of the detection event in terms of v_j`s, we have $X = v_0$ and $Y = \sum_{j=1}^{N-1} v_j$. The MGF of $X$ is just the MGF of $v_0$, and the MGF of $Y$ is just the product of the MGF`s of the v_j`s, j = 1,...,N-1:

$$h_X(u) = \frac{1}{(1+\sigma^2 u)} \exp\left\{ \frac{-\frac{1}{2}|A\mathbf{h}^{\dagger}\mathbf{s}|^2 u}{1+\sigma^2} \right\} \tag{3.32}$$

$$h_Y(u) = \prod_{j=1}^{N-1} \frac{1}{(1+\sigma^2 u)} \exp\left\{ \frac{\frac{-1}{2}|A\phi_j^{\dagger}\mathbf{s}|^2 u}{1+\sigma^2 u} \right\} \tag{3.33}$$

It is interesting to note that the MGF of X depends on only A^2, ρ^2, σ^2. The MGF of Y depends only on σ^2 and the energy in the signal vector in the directions other than **h**. This means that the detection probabilities do not depend directly on the codes and filter of the system but only on the ρ, and thus the ρ_j, that they produce.

By subtracting tY from both sides detection event can be expressed as comparing a Chi-squared random variable to a deterministic threshold,

$$P = P_r[X > tY] = P_r[X - tY > 0] \tag{3.34}$$

This probability function is just one minus the cdf of a random variable. Since the MGF is known, P is computed by solving the contour integration problem,

$$P = \int_{C^-} (-u)^{-1} h_X(u) h_Y(-tu) \frac{du}{2\pi j} \tag{3.35}$$

Thus we obtain the probability of detection event as a function of a constant false alarm rate.

We shall subsequently use these results for designing and analyzing our new algorithm.

3.3 Truncated Sequential Probability Ratio Test

In the previous section we have discussed the CFAR form of signal detection. In this section we will discuss another form of signal detection which will be used for user specific code acquisition within each multipath. Among the three most common decision rules – Bayes, minimax and Neyman-Pearson, we would choose Neyman-Pearson [45] criteria because the least *a-priori* knowledge is required, in which a bound is placed on the false-alarm probability and the probability of detection is maximised within this constraint [46] [47]. TSPRT is a mixture of FSS and SPRT. Hence in the following sections, FSS hypothesis testing, sequential detection and MHT will be analysed.

3.3.1 Fixed Sample Size Test

The basic physical observation model that we wish to consider is an observed waveform that consists of possible signal presence corrupted by additive noise and our objective is to decide

whether the signal is present or not by processing a collection of samples with observation window size N taken from the observed waveform.

Suppose the signal in (3.24) has constant amplitude and has a Gaussian distribution, we want to test a positive shift in the mean [48]. Let $\mathbf{y} \equiv y_1, y_2, \ldots$ be realizations of (i.d.d) random variables $\mathbf{Y} \equiv Y_1, Y_2, \ldots$. We denote θ as the common mean of each of the Y_i's. Consider testing the hypothesis H_0, under which Y_i has a pdf $f(y-\theta_0)$, against a shifted alternative H_1; that is, consider the hypothesis pair:

$$H_0 : Y_i \sim f(y-\theta), \theta = \theta_0$$

versus

$$H_1 : Y_i \sim f(y-\theta), \theta = \theta_1 > \theta_0$$

for all i, where $f(y_i)$ is the Gaussian probability density function of Y_i with variance υ^2. The Neyman-Pearson (NP) FSS test is obtained by testing N samples and the log likelihood function $L(y)$ [45]:

$$L(y) = \sum_{i=1}^{N} z_i \begin{cases} \geq \tau \Rightarrow choose H_1 \\ < \tau \Rightarrow choose H_0 \end{cases}$$

where z_i is the observed realization of the random variable

$$Z_i = \ln\left[\frac{f(y_i-\theta_1)}{f(y_i-\theta_0)}\right] = (\theta_1-\theta_0)(Y_i-(\theta_1+\theta_0)/2)/\upsilon^2 \qquad (3.36)$$

Since we consider Gaussian distribution for the decision variable, hence we determine the first and second moments. The first moment of the Z_i given θ is

$$\begin{aligned}\mu_\theta &\equiv E(Z_i \mid \theta) \\ &= \int \ln\left[\frac{f(y_i-\theta_1)}{f(y_i-\theta_0)}\right] f(x-\theta)dx \\ &= (\theta_1-\theta_0)^2 (r-\tfrac{1}{2})/v^2\end{aligned} \tag{3.37}$$

where $r = (\theta-\theta_0)/(\theta_1-\theta_0)$. The second moment is

$$\begin{aligned}m_\theta &\equiv E(Z_i^2 \mid \theta) \\ &= \int \left\{\ln\left[\frac{f(y_i-\theta_1)}{f(y_i-\theta_0)}\right]\right\}^2 f(x-\theta)dx \\ &= \left(\frac{\theta_1-\theta_0}{v}\right)^2 + \frac{(\theta_1-\theta_0)^4(r-\frac{1}{2})^2}{v^4}\end{aligned} \tag{3.38}$$

and the conditional variance is

$$\sigma_\theta^2 \equiv m_\theta - \mu_\theta^2 = \left(\frac{\theta_1-\theta_0}{v}\right)^2 \equiv \sigma^2 \tag{3.39}$$

To reduce subscripts we define $\mu_1 \equiv \mu_{\theta_1}$ and $\mu_0 \equiv \mu_{\theta_0}$. Then we have

$$\mu_0 = -(\theta_1-\theta_0)^2/2v^2 = -\mu_1 \tag{3.40}$$

The sample size N and the threshold τ are pre-chosen [48]so that the test has error probabilities P(choosing $H_1 \mid H_0$ true) and P(choosing $H_0 \mid H_1$ true) of a and 1-β determine the threshold, τ,

$$\tau = N^{1/2}[\mu_1\Psi^{-1}(\alpha) + \mu_0\Psi^{-1}(1-\beta)](\sigma/(\mu_0-\mu_1)) \tag{3.41}$$

and number of test samples,

$$N = [\Psi^{-1}(\alpha) + \Psi^{-1}(1-\beta)]^2 (\sigma/(\mu_1-\mu_0))^2 \tag{3.42}$$

where $\Psi(\bullet)$ represents the standard (normalized) Gaussian distribution function and $\Psi^{-1}(\bullet)$ is its inverse [48].

3.3.2 Sequential Detection

We will now see a different type of hypothesis where we will carry out hypothesis testing over each chip and truncate the test once we achieve the required level of confidence. Unlike the FSS test, there is an alternative approach where the desired performance is fixed and the number of samples is allowed to vary in order to achieve this performance. Namely for some realizations of the observation sequence we may be able to make a decision after only a few samples, whereas for some other realizations we may wish to continue sampling to make a better decision. A detection scheme that uses a random number of samples depending on the observation sequence is generally known as sequential detection. Wald's [49] sequential probability ratio test is obtained by testing, at the nth sample.

$$\sum_{i=1}^{n} z_i \begin{cases} < B \quad \Rightarrow H_0 \;\; P(z_1, z_2, \ldots, z_n) \\ > \mathrm{A} \quad \Rightarrow H_1 \\ \in (B, A) \Rightarrow \text{ take another sample,} \end{cases} \tag{3.43}$$

where the boundaries A and B are chosen so that the error probabilities are α and 1-β. The sample size $M = \min\{n : \sum_{i=1}^{n} z_i \notin (B, A)\}$ is now a random variable, and average sample number depends on the actual distribution of Z_i, i = 1, 2, 3,…., which depends on the value of θ. This can be represented diagrammatically as shown in Figure 3.5.

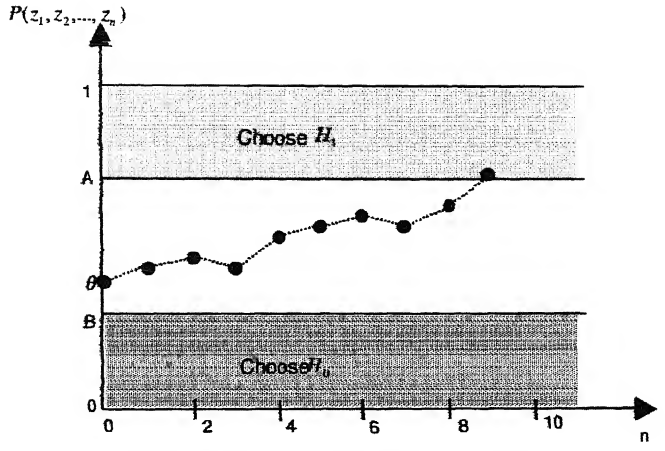

Figure 3.5: Depiction of Sequential Detection

The main benefits of using the sequential probability ratio test (SPRT) lie in the following three facts:

- Sequential detection achieves same probability of false alarm and detection as a fixed length test.
- The average test length for the sequential detection is smaller than for a fixed length test.
- The reduced average test length can be exploited to reduce computation complexity.

An obvious disadvantage of the SPRT is that occasional long tests may result if the observed data are ambiguous. As the Wald-Wolfowitz theorem [46] implies the average test length of SPRT is much shorter than FSS. However, these occasional long runs may not be practical for many applications. A practical compromise is a truncated SPRT (T-SPRT) where a finite-stage truncation exists [48]. As a trade-off, the optimality property in terms of minimizing average sample size (ASS) is lost by such a truncation. Nevertheless, the increase in ASS is usually slight. In the truncation stage, $n = M^*$, test

$$\sum_{i=1}^{M^*} z_i \quad \begin{cases} < t^* \Rightarrow H_0 \\ \geq t^* \Rightarrow H_1 \end{cases} \tag{3.44}$$

3.3.3 Multistage Hypothesis Test

In the section on Sequential Detection we have seen the T-SPRT was expressed in terms of the log likelihood function, which is impractical for realistic system design. In terms of the received samples, the T-SPRT can be rewritten as [47]:

$$\sum_{i=1}^{n} y_i \quad \begin{cases} < B_n \text{ choose } H_0 \text{ and terminate} \\ > A_n \text{ choose } H_1 \text{ and terminate} \\ \text{else continue to stage n+1} \end{cases} \tag{3.45}$$

in stage n, $1 \leq n \leq N_t$. At the N_t th stage, we test

$$\sum_{i=1}^{n} y_i \quad \begin{cases} \geq A_N \Rightarrow chooseH_1 \\ else \Rightarrow chooseH_0 \end{cases} \tag{3.46}$$

where the A_n and B_n are thresholds at the stage n and N_t is the truncation stage. In the following, we give the transformation step by step.

$$\begin{aligned} \sum_{i=1}^{n} z_i = \sum_{i=1}^{n} (\theta_1 - \theta_0)(Y_i - (\theta_1 + \theta_0)/2)/v^2 \quad & \text{vs} \quad A \\ \equiv \sum_{i=1}^{n} (Y_i - (\theta_1 + \theta_0)/2) \quad & \text{vs} \quad \frac{Av^2}{(\theta_1 - \theta_0)} \\ \equiv \sum_{i=1}^{n} y_i \quad & \text{vs} \quad \frac{Av^2}{(\theta_1 - \theta_0)} + \sum_{i=1}^{n} \frac{(\theta_1 + \theta_0)}{2} \\ \equiv \sum_{i=1}^{n} y_i \quad & \text{vs} \quad \frac{Av^2}{(\theta_1 - \theta_0)} + \frac{n(\theta_1 + \theta_0)}{2} \end{aligned} \tag{3.47}$$

Here we define the upper threshold at stage n as:

$$A_n \equiv \frac{A\upsilon^2}{(\theta_1-\theta_0)}+\frac{n(\theta_1+\theta_0)}{2} \tag{3.48}$$

Similarly, the lower threshold at stage n can be expressed as:

$$B_n \equiv \frac{B\upsilon^2}{(\theta_1-\theta_0)}+\frac{n(\theta_1+\theta_0)}{2} \tag{3.49}$$

where $1 \le n \le N_t$ and the truncation threshold at stage N_t can be expressed as:

$$A_{N_t} = \frac{\tau\upsilon^2}{(\theta_1-\theta_0)}+\frac{N_t(\theta_1+\theta_0)}{2} \tag{3.50}$$

From equations (3.48), (3.49) and (3.50), the $2N_t-1$ parameters for an N_t-stage test are reduced to four parameters: A, B, truncation point τ and truncation stage N_t. The T-SPRT can be viewed as a mixture of SPRT and FSS tests. If c_0 and c_1 are mixing constants each on [0,1], using Wald's inequalities [46, 48], we set

$$\hat{A} = \ln\left[\frac{1-(1-c_1)P_M}{(1-c_0)P_F}\right] \tag{3.51}$$

$$\hat{B} = \ln\left[\frac{(1-c_1)P_M}{1-(1-c_0)P_F}\right] \tag{3.52}$$

$$N_t = \left[\Psi^{-1}(c_0P_F)+\Psi^{-1}(c_1P_M)\right]^2\left(\frac{\sigma}{\mu_1-\mu_0}\right)^2 \tag{3.53}$$

and

$$\tau = \sqrt{N_t}\left[\mu_1\Psi^{-1}(c_0P_F)+\mu_0\Psi^{-1}(c_1P_M)\right]\left(\frac{\sigma}{\mu_0-\mu_1}\right) \tag{3.54}$$

where $P_F = \alpha$, and $P_M = 1-\beta$.

The design may be optimised by varying c_0 and c_1: values of c_0 and c_1 near 0 yields a test similar to SPRT. Alternatively, values of c_0 and c_1 near 1 may result in similarity to an FSS test. In the test design, σ, μ_0, and μ_1 are known; P_F and P_M are nominally chosen design values of the error probabilities. Once c_0 and c_1 are chosen, test is completely specified by $\hat{A}, \hat{B}, N_t$ and τ. The

design guarantees that for independent and identically distributed samples; the actual probability of false alarm and missed detection will be lower than nominal values. The performance of the MHT will be carried out subsequently. We shall analyse the probability of MHT reaches a certain stage and the probability of accepting either hypothesis.

3.3.4 MHT for Rayleigh Fading Channel

We shall now extend MHT for reception of Rayleigh faded signals at the output of a correlator. By Central Limit theorem, the pdf of the output of the correlator, when there are number of users will have a Gaussian distribution. Moreover, if the signal has undergone Rayleigh fading, then the joint distribution at the output of the correlator will be a combination of Rayleigh and Gaussian distribution.

The pdf of the amplitude of the received waveform is Rayleigh distributed. The chip energy E_c is multiplied by ς^2 where ς is Rayleigh distributed. Hence,

$$f_R(\varsigma) = \frac{2\varsigma}{\sigma_R^2} \exp\left(\frac{-\varsigma^2}{\sigma_R^2}\right), \varsigma \geq 0 \tag{3.55}$$

where $\sigma_R^2 = E[\varsigma^2]$ and $E[\cdot]$ is the expectation operator. Let $\gamma = \varsigma^2$ then we have

$$f_R(\gamma) = \frac{1}{\sigma_R^2} \exp\left(\frac{-\gamma}{\sigma_R^2}\right) \tag{3.56}$$

where $f_R(\gamma)$ is the pdf for Rayleigh distribution, σ_R is the variance of the distribution. The average chip energy becomes

$$\overline{E}_c = \overline{\varsigma}^2 E_c = \overline{\gamma} E_c = \sigma_R^2 E_c \tag{3.57}$$

At the output of the correlator, we now have the following situations:

- Under H_0 hypothesis, there are two possibilities:
    - there is no signal, the pdf is zero-mean Gaussian
    - there is Rayleigh faded signal that is uncorrelated at the output of the correlator

- Under H_1 hypothesis, the Rayleigh faded signal is present and it is correlated at the output of the correlator.

Under null hypothesis and in the first case, it is a pure noise-only path that causes the thresholds to be higher while in the second case, the Rayleigh faded signal is present but uncorrelated at the output of the correlator causing the thresholds to be lower. As will be seen later, in our system we shall use two level of detection and the MHT will be used in the second stage detector provided the first detector (CFAR) decides that a signal is present. Moreover, in the uplink, there will be some or the other baseband signal present and hence we reject the no signal case. For the analysis of MHT in the case of Rayleigh fading, we consider only the second case under null hypothesis.

Then as given in [9] the pdf considered in section 3.3.1 for the Gaussian case will now be modified by weighing the signal power or equivalently θ_i by γ. Then we have

$$\begin{aligned} H_0 : Y_i &\sim \frac{1}{\sigma_R^2}\exp\left(\frac{-\gamma}{\sigma_R^2}\right) f(y-\gamma\theta), \theta = \theta_0 \\ H_1 : Y_i &\sim \frac{1}{\sigma_R^2}\exp\left(\frac{-\gamma}{\sigma_R^2}\right) f(y-\gamma\theta), \theta = \theta_1 > \theta_0 \end{aligned} \tag{3.58}$$

The NP test variable will now be given by

$$\begin{aligned} Z_i &= \ln\left[\frac{f(y_i-\theta_1)}{f(y_i-\theta_0)}\right] \\ &= \ln\left[\frac{\frac{1}{\sigma_R^2}\exp\left(\frac{-\gamma}{\sigma_R^2}\right)\frac{1}{\sqrt{2\pi}\upsilon}\exp\left(\frac{-(y_i-\gamma\theta_1)^2}{2\upsilon^2}\right)}{\frac{1}{\sigma_R^2}\exp\left(\frac{-\gamma}{\sigma_R^2}\right)\frac{1}{\sqrt{2\pi}\upsilon}\exp\left(\frac{-(y_i-\gamma\theta_0)^2}{2\upsilon^2}\right)}\right] \\ &= \frac{\gamma}{\upsilon^2}(\theta_1-\theta_0)\left(Y_i - \frac{\gamma(\theta_1+\theta_0)}{2}\right) \end{aligned} \tag{3.59}$$

The difference between the Gaussian NP decision variable in (3.36) and the joint Rayleigh and Gaussian variable in (3.59) is the multiplication by the factor γ. Accordingly, (3.47) will now be modified as:

$$\sum_{i=1}^{n} z_i \equiv \sum_{i=1}^{n} y_i \qquad \text{vs} \qquad \frac{A\upsilon^2}{\gamma(\theta_1-\theta_0)}+\frac{n\gamma(\theta_1+\theta_0)}{2} \tag{3.60}$$

The upper threshold for stage n gets modified as:

$$A_n \equiv \frac{A\upsilon^2}{\gamma(\theta_1-\theta_0)}+\frac{n\gamma(\theta_1+\theta_0)}{2} \tag{3.61}$$

and the lower threshold gets modified as:

$$B_n \equiv \frac{B\upsilon^2}{\gamma(\theta_1-\theta_0)}+\frac{n\gamma(\theta_1+\theta_0)}{2} \tag{3.62}$$

The truncation stage threshold is given by:

$$A_{N_t} = \frac{\tau\upsilon^2}{\gamma(\theta_1-\theta_0)}+\frac{N_t\gamma(\theta_1+\theta_0)}{2} \tag{3.63}$$

Next, we analyse the changes occurring to the mean, mean square and variance of the decision variable Z_i given in (3.37), (3.38) and (3.39) respectively. The first moment of Z_i for a given θ is:

$$\begin{aligned}
\mu_\theta \equiv E(Z_i/\theta) &= E\left\{\frac{\gamma}{\upsilon^2}(\theta_1-\theta_0)\left(Y_i-\frac{\gamma(\theta_1+\theta_0)}{2}\right)\right\} \\
&= \frac{\gamma}{\upsilon^2}(\theta_1-\theta_0)E\left(Y_i-\frac{\gamma(\theta_1+\theta_0)}{2}\right) \\
&= \frac{\gamma}{\upsilon^2}(\theta_1-\theta_0)\left(\theta-\frac{\gamma(\theta_1+\theta_0)}{2}\right) \\
&= \frac{\gamma}{\upsilon^2}(\theta_1-\theta_0)^2\left(r-\frac{\gamma}{2}\right)
\end{aligned} \tag{3.64}$$

where $r=(\theta-\gamma\theta_0)/(\theta_1-\theta_0)$. The second moment is given by:

$$m_\theta \equiv E\left(Z_i^2/\theta\right) = E\left[\left(\frac{\gamma}{v^2}(\theta_1-\theta_0)\left(Y_i - \frac{\gamma(\theta_1+\theta_0)}{2}\right)\right)^2\right]$$

$$= \frac{\gamma^2}{v^4}(\theta_1-\theta_0)^2 E\left(Y_i^2 - Y_i\gamma(\theta_1+\theta_0) + \frac{\gamma^2(\theta_1+\theta_0)^2}{4}\right)$$

$$= \frac{\gamma^2}{v^4}(\theta_1-\theta_0)^2\left(v^2+\theta^2\right) + \frac{\gamma^2}{v^4}(\theta_1-\theta_0)^2\left(-\theta\gamma(\theta_1+\theta_0) + \frac{\gamma^2(\theta_1+\theta_0)^2}{4}\right)$$

$$\left[\because E\left[Y_i^2\right] = \left(v^2+\theta^2\right)\right]$$

$$= \frac{\gamma^2}{v^2}(\theta_1-\theta_0)^2 + \frac{\gamma^2}{v^4}(\theta_1-\theta_0)^2\left(\theta^2 - \theta\gamma(\theta_1+\theta_0) + \frac{\gamma^2(\theta_1+\theta_0)^2}{4}\right)$$

$$= \frac{\gamma^2}{v^2}(\theta_1-\theta_0)^2 + \frac{\gamma^2}{v^4}(\theta_1-\theta_0)^2\left(\theta - \frac{\gamma(\theta_1+\theta_0)}{2}\right)^2 \qquad (3.65)$$

$$= \frac{\gamma^2}{v^2}(\theta_1-\theta_0)^2 + \frac{\gamma^2}{v^4}(\theta_1-\theta_0)^4\left(r - \frac{\gamma}{2}\right)^2$$

The conditional variance is modified from (3.39) and given by:

$$\sigma^2 \equiv m_\theta - \mu_\theta^2$$

$$= \frac{\gamma^2}{v^2}(\theta_1-\theta_0)^2 + \frac{\gamma^2}{v^4}(\theta_1-\theta_0)^4\left(r-\frac{\gamma}{2}\right)^2 - \left(\frac{\gamma}{v^2}(\theta_1-\theta_0)^2\left(r-\frac{\gamma}{2}\right)\right)^2 \qquad (3.66)$$

$$= \frac{\gamma^2}{v^2}(\theta_1-\theta_0)^2$$

The modified values of μ_θ and σ^2 from(3.64) and (3.66) can be used in (3.53) and (3.54) for obtaining the values of N_t and τ.

Chapter 4

Proposed Algorithm for Code Acquisition

4.1 Introduction

Parallel code acquisition schemes are computationally intensive. Here we propose a new algorithm for parallel code acquisition in uplink WCDMA which has lower computational complexity. A searcher is employed by the Rake receiver to detect different multipaths in order to provide multipath diversity for the traffic channels. The BS provides the timing adjustment information to the MS [1]. This ensures that the multipath signals from different MS arrive at the BS at close intervals. We first carryout non-coherent joint detection of multipath signals at the BS using CFAR technique. For this we concatenate the existing scrambling code of different MS with length 13 Barker sequence. The Barker sequence concatenated signals of different MS with same relative delay are jointly detected at the BS by a CMF matched to the Barker sequence. Then in each detected delay-path, we carryout user-specific coherent code acquisition by tree search.

4.2 Tree Search Algorithm

The number of CMFs for parallel search employing brute force approach would be number of users multiplied by the number of possible phases for each user. Instead we propose an alternate method of code acquisition. This algorithm uses the short spreading codes of existing users to construct a binary tree and then the tree is pruned breadth first for code acquisition using TSPRT. This has lower computational complexity since TSPRT requires much lesser number of samples than a FSS test [49].

4.2.1 Code Tree Construction

Instead of testing all possible circular shifts of all users PN codes independently by a bank of correlators/CMFs, we propose to test them jointly and utilize common testing statistics. Some shifts of PN codes have initial chips in common; simultaneous hypothesis testing is possible by organizing all users PN codes into a code tree. This is achieved by first enumerating all possible PN codes with all possible circular phase shifts of existing users in a code book. Then we proceed through the codebook, codeword by codeword. Each codeword is processed chip by chip: each chip value is encoded in a code tree node.

In a WCDMA uplink system, let us consider K users existing. Let codebook C denote a matrix with K rows. Each row corresponds to a user in the system with length N chips where N is the length of test. For the convenience of algorithm description, we identify each node at a particular depth level of the tree search by the rule:

- **Node (i, j) denotes the j^{th} tree node at tree depth level i.**
- **Node (i, j)'s left child is labeled as node $(i+1, 2j-1)$.**
- **Node (i, j)'s right child is labeled as node $(i+1, 2j)$.**
- $i = 1,\ldots\ldots,N$, $1 \le j \le 2^i$, where N is the number of chips over which the TSPRT test is carried out.

The sequential detection test can be done independently.

The procedure of constructing the code tree works recursively. The chip values of codebook C are labeled row by row according to the labeling rule. For row i, chip j:

- **If $C[i][j] = -1$, then generate a left child**

- **If $C[i][j] = 1$, then generate a right child**

The last row of the codebook consists of K^{th} leaf nodes of the tree, i.e., no children are generated at the end of each row. The depth of the tree is, therefore, N level.

The problem with this system of code acquisition is that at the early stages of the sequential test if a rejection occurs, then a large part of the tree is not searched and this leads to higher missed detection. At the same time if a selection occurs at an early stage, it will lead to a higher false alarm. We will suggest an alternative method of tree search which will reduce both the miss detection and false alarms and also limit the size of the codebook. In order to limit the false alarm rate and miss detection, we will restrict the size of the codebook. This is achieved by constructing the codebook only for existing users with zero circular phase shifts. We then carry out a two level search – first we have non-coherent detection of different multipaths that are existent in the uplink system and then we carryout coherent tree search within each delay path. For this we concatenate the short spreading codes of all users with Barker sequences which have got excellent autocorrelation properties and can resolve multipath. As per the existing WCDMA standards [1], in the uplink the BS gives timing adjustment command to the MS to adjust its transmit time. The timing resolution should be within 1.5 T_c [1]. This implies that multipaths of different users with comparable relative delays will arrive at the BS at close intervals and therefore make code acquisition by joint detection feasible.

4.3 Joint Multipath Detection

Barker sequences have excellent autocorrelation properties that can be utilized for multipath detection. The same is explained in the next section.

4.3.1 Barker Sequences and its Properties

We define Barker Sequence as a sequence $\{a_r\}$ of +1's and –1's of some finite length k such that the correlation function $C(\tau)$ defined by [50]

$$C(\tau) = \sum_{r=1}^{k-\tau} a_r a_{r+\tau}^{*} \text{ satisfies } |C(\tau)| \le 1 \text{ for } \tau \neq 0. \tag{4.1}$$

In (4.3) we have given the expression for the aperiodic autocorrelation function. We now define the periodic or the even autocorrelation function (EAC) as:

$$\theta(\tau) = C(\tau) + C^{*}(N_B - \tau) \tag{4.2}$$

and the odd autocorrelation function (OAC) as:

$$\hat{\theta}(\tau) = C(\tau) - C^{*}(N_B - \tau) \tag{4.3}$$

where N_B is the length of the Barker Sequence. The OAC function affects the output of the Correlator when the information symbols change over one integration interval, while the EAC function affects the output when the information symbols do not change. Thus, when the binary information symbols are equiprobable, both the EAC and OAC functions are equally important in the system design and performance analysis. In addition to the above two properties there are two other interesting properties. Namely, the Merit Factor – which specifies the ratio of energy of the ACF main lobe to the energy in the ACF side lobes

$$MF = \frac{C^2(0)}{\sum_{m=1}^{N_B-1} |C(m)|^2} \tag{4.4}$$

and the HNV which specifies the ratio of the ACF value at m = 0 to the ACF out-of-phase value with maximum absolute value

$$HNV = \frac{C(0)}{C_a} \qquad \forall m \neq 0 \bmod N_B \tag{4.5}$$

$$\text{and } C_a = \max_{1 \le \tau < N_B} \{C(\tau)\}. \tag{4.6}$$

There are a total of six binary Barker sequences. For our algorithm we shall use length 13 Barker sequence which will cater for a delay spread of 13 chip-time. The sequences and its correlation properties is as shown in the Table 4.1 and Figure 4.1. This is very important from our point of view since Barker sequences have a very good merit factor and their *HNV* equals the length *N*. This gives a measure that by how much will the in-phase components is above the out-of-phase components. The highest known merit factor of 14.08 is that of length 13 sequence. The correlation properties of binary Barker sequence of length 13 are as shown in Figure 4.1.

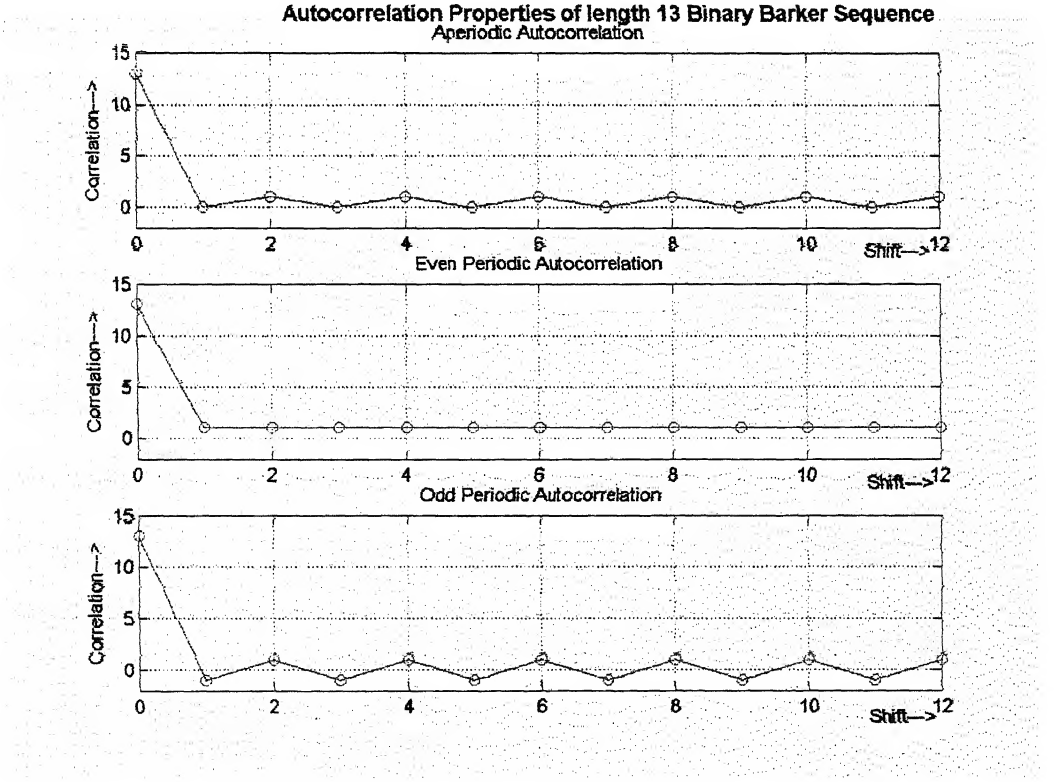

Figure 4.1: Correlation properties of Barker Sequence of length 13.

N_B	Barker Sequence and Properties	MF
13	Seq: {+1, +1, +1, +1, +1, -1, -1, +1, +1, -1, +1, -1, +1}	14.08
	ACF: (13, 0, 1, 0, 1, 0, 1, 0, 1, 0, 1, 0, 1)	
	PCF: (13, 1, 1, 1, 1, 1, 1, 1, 1, 1, 1, 1, 1)	
	OCF:(13, -1, 1, -1, 1, -1, 1, -1, 1, -1, 1, -1, 1)	

Table 4.1: Correlation properties of binary Barker Sequences

4.3.2 Concatenation of Short Spreading Codes by Barker Sequence

In the previous section we have seen the excellent correlation properties possessed by the Barker sequences. These sequences can be used to detect multipaths over smaller number of chips. When the received signal is passed through a Barker correlator the output at the zero time-shift is 13 dB higher than other shifts of a length 13 Barker sequence. Thus, it will be possible to detect the different multipath signals with the help of Barker sequences.

Let us denote the length 13 Barker sequence by the vector

$$\{\hat{b}_n\} = (1,1,1,1,1,-1,-1,1,1,-1,1,-1,1) \tag{4.7}$$

for $n = 1, 2, \ldots, 13$. The $\{c_n^{(i)}\}$ in section 2.7.1, which is the scrambling sequence, will be modified and represented as:

$$\{c_n'^{(i)}\} = (\hat{b}_{n_b}, \hat{c}_{n_f}^{(i)}, \hat{b}_{n_b-128}, \hat{c}_{n_l}^{(i)}) \tag{4.8}$$

where $1 \le n_b \le 13$, $14 \le n_f \le 128$, $142 \le n_l \le 256$.

The transmitted digital spread spectrum signal from user i in one symbol interval can now be represented by:

$$s_i(n) = c_n'^{(i)} d_i \tag{4.9}$$

The received baseband discrete-time signal in one symbol period is obtained from (2.10), (4.8) and (4.9) as:

$$r(n) = \sum_{i=1}^{K}\sum_{j=1}^{L} \beta_{ij} d_i c^{(i)}_{n-\tau_{ij}} + z(n) \tag{4.10}$$

This received baseband signal is passed through a CMF matched to Barker sequence with delay of p chips. The discrete-time output of the Barker CMF in one symbol period when M users have paths with delay of p chips is given by:

$$\begin{aligned}
Z_p &= \sum_{n=1}^{N_B} r(n)\hat{b}_{n-\tau_p} \\
&= \sum_{n=1}^{N_B}\sum_{i=1}^{K}\sum_{j=1}^{L}\left(\left(\hat{b}_{n_b-\tau_j}, \hat{c}^{(i)}_{n_f-\tau_{ij}}, \hat{b}_{n_b-128-\tau_j}, \hat{c}^{(i)}_{n_l-\tau_{ij}}\right)\beta_{ij} + w(n)\right)\hat{b}_{n-\tau_p} \\
&= \sum_{n=1}^{N_B}\sum_{i=1}^{M} \beta_{ip}\left(\delta(n-\tau_p) + \delta(n-128-\tau_p)\right) \\
&\quad + \sum_{n=1}^{N_B}\sum_{k=1}^{K}\sum_{\substack{l=1 \\ kl\neq ip}}^{L}\left(\left(\hat{c}^{(k)}_{n_f-\tau_{kl}} + \hat{c}^{(k)}_{n_l-\tau_{kl}} + \hat{b}_{n_b-\tau_l} + \hat{b}_{n_b-128-\tau_l}\right)\beta_{kl} + z(n)\right)\hat{b}_{n-\tau_p} \\
&= C(0)\sum_{i=1}^{M}\left(\beta_{ip}\left(\delta(n-\tau_p) + \delta(n-128-\tau_p)\right)\right) \\
&\quad + \sum_{k=1}^{K}\sum_{\substack{l=1 \\ kl\neq ip}}^{L}\left(\left(\rho^{(k)}_{lp} + C(\tau)\delta(n-\tau_l) + C(\tau)\delta(n-128-\tau_l)\right)\beta_{kl} + z(n)\hat{b}_{n-\tau_p}\right) \\
&\cong N_B\sum_{i=1}^{M}\left(\beta_{ip}\left(\delta(n-\tau_p) + \delta(n-128-\tau_p)\right)\right) \\
&\quad + \sum_{k=1}^{K}\sum_{\substack{l=1 \\ kl\neq ip}}^{L}\left(\left(\rho^{(k)}_{lp} + C(\tau)\delta(n-\tau_l) + C(\tau)\delta(n-128-\tau_l)\right)\beta_{kl} + z(n)\hat{b}_{n-\tau_p}\right) \\
&\cong N_B\sum_{i=1}^{M}\left(\beta_{ip}\left(\delta(n-\tau_p) + \delta(n-128-\tau_p)\right)\right) + IN_p
\end{aligned} \tag{4.11}$$

where $$IN_p = \sum_{k=1}^{K}\sum_{\substack{l=1 \\ kl\neq ip}}^{L}\left(\left(\rho^{(k)}_{lp} + C(\tau)\delta(n-\tau_l) + C(\tau)\delta(n-128-\tau_l)\right)\beta_{kl} + z(n)\hat{b}_{n-\tau_p}\right) \tag{4.12}$$

is the resulting interference and

$$\rho^{(k)}_{lp} = \left(\hat{c}^{(k)}_{n_f-\tau_{kl}} + \hat{c}^{(k)}_{n_l-\tau_{kl}}\right)\hat{b}_{n-\tau_p} \tag{4.13}$$

is the cross-correlation between Barker sequence and the scrambling code. The first term in (4.11) is due to the exact match resulting from a total of M users with the same time delay of p

chips. The second term is due to the balance of *K-M* users with path delays not matched to the CMF.

Comments: The following are observed:

- The first term will be 13 dB higher than the second term with the $C(\tau)$ terms and has been seen in the properties of Barker sequence.
- The cross-correlation term $\rho_{lp}^{(k)}$ in (4.13) can have a normalised value in the range [0, 1]. This means that even in the case when there is no exact match, this term could lead to situations of false detection. Thus, there is a need to reduce this cross-correlation term.

4.3.3 Decorrelated and Concatenated Sequence

In this section we will address the problem of reduction of cross-correlation as given in (4.13). We shall now carryout modification on the concatenated sequence given in (4.8).

In order to reduce the cross-correlation between Barker sequence and the scrambling sequence, we will decorrelate the scrambling sequence part ($\hat{c}_{n_f}^{(i)}$ and $\hat{c}_{n_t}^{(i)}$). This is achieved by decorrelating the original scrambling sequence at the transmitter with a filter that satisfies the following criteria:

$$\hat{b}_n \hat{a}_n = 1$$
$$\hat{b}_n \hat{a}_n \hat{b}_n = \hat{b}_n .$$
$$\hat{a}_n \hat{b}_n \hat{a}_n = \hat{a}_n$$

Such a filter is given by:

$$\{\hat{a}_n\}^T = (0.076923, 0.076923, 0.076923, 0.076923, 0.076923, -0.076923, -0.076923, 0.076923, 0.076923, -0.076923, 0.076923, -0.076923, 0.076923) \quad (4.14)$$

The de-correlated and concatenated sequence can now be represented as:

$$\left\{c_n^{"(i)}\right\} = \left(\hat{b}_{n_b}, \hat{c}_{n_f}^{(i)} * \hat{a}_n, \hat{b}_{n_b-128}, \hat{c}_{n_l}^{(i)} * \hat{a}_n\right) \tag{4.15}$$

where * represents convolution. The equations (4.9) and (4.10) will now be given by:

$$s_i(n) = c_n^{"(i)} d_i \tag{4.16}$$

$$r(n) = \sum_{i=1}^{K}\sum_{j=1}^{L} \beta_{ij} d_i c_{n-\tau_{ij}}^{"(i)} + z(n) \tag{4.17}$$

For the same given conditions as in section 4.3.2, we now have:

$$\begin{aligned}
Z_p &= \sum_{n=1}^{N_B} r(n)\hat{b}_{n-\tau_p} \\
&= \sum_{n=1}^{N_B}\sum_{i=1}^{K}\sum_{j=1}^{L}\left(\left(\hat{b}_{n_b-\tau_j}, \hat{c}_{n_f-\tau_{ij}}^{(i)} * \hat{a}_{n-\tau_j}, \hat{b}_{n_b-128-\tau_j}, \hat{c}_{n_l-\tau_{ij}}^{(i)} * \hat{a}_{n-\tau_j}\right)\beta_{ij} + w(n)\right)\hat{b}_{n-\tau_p} \\
&= \sum_{n=1}^{N_B}\sum_{i=1}^{M} \beta_{ip}\left(\delta(n-\tau_p) + \delta(n-128-\tau_p)\right) \\
&\quad + \sum_{n=1}^{N_B}\sum_{k=1}^{K}\sum_{\substack{l=1 \\ kl\neq ip}}^{L}\left(\left(\hat{c}_{n_f-\tau_{kl}}^{(k)} * \hat{a}_{n-\tau_j} + \hat{c}_{n_l-\tau_{kl}}^{(k)} * \hat{a}_{n-\tau_j} + \hat{b}_{n_b-\tau_l} + \hat{b}_{n_b-128-\tau_l}\right)\beta_{kl} + z(n)\right)\hat{b}_{n-\tau_p} \\
&= C(0)\sum_{i=1}^{M}\left(\beta_{ip}\left(\delta(n-\tau_p) + \delta(n-128-\tau_p)\right)\right) \\
&\quad + \sum_{k=1}^{K}\sum_{\substack{l=1 \\ kl\neq ip}}^{L}\left(\left(\sum_{n=1}^{N_B}\left(\hat{c}_{n_f-\tau_{kl}}^{(k)} * \hat{a}_{n-\tau_j} + \hat{c}_{n_l-\tau_{kl}}^{(k)} * \hat{a}_{n-\tau_j}\right)\hat{b}_{n-\tau_p} + C(\tau)\delta(n-\tau_l) + C(\tau)\delta(n-128-\tau_l)\right)\beta_{kl} + z(n)\,\hat{b}_{n-\tau_p}\right) \\
&\cong N_B\sum_{i=1}^{M}\left(\beta_{ip}\left(\delta(n-\tau_p) + \delta(n-128-\tau_p)\right)\right) \\
&\quad + \sum_{k=1}^{K}\sum_{\substack{l=1 \\ kl\neq ip}}^{L}\left(\left(\rho_{lp}^{(k)} + C(\tau)\delta(n-\tau_l) + C(\tau)\delta(n-128-\tau_l)\right)\beta_{kl} + z(n)\hat{b}_{n-\tau_p}\right) \\
&\cong N_B\sum_{i=1}^{M}\beta_{ip}\left(\delta(n-\tau_p) + \delta(n-128-\tau_p)\right) + IN_p
\end{aligned} \tag{4.18}$$

$$\text{where } IN_p = \sum_{k=1}^{K} \sum_{\substack{l=1 \\ kl \neq ip}}^{L} \left(\left(\rho_{lp}^{(k)} + C(\tau)\delta(n-\tau_l) + C(\tau)\delta(n-128-\tau_l) \right) \beta_{kl} + z(n)\hat{b}_{n-\tau_p} \right) \tag{4.19}$$

$$\text{and } \rho_{lp}^{(k)} = \sum_{n=1}^{N_B} \left(\hat{c}_{n_j-\tau_{kl}}^{(k)} * \hat{a}_{n-\tau_j} + \hat{c}_{n_l-\tau_{kl}}^{(k)} * \hat{a}_{n-\tau_j} \right) \hat{b}_{n-\tau_p} \tag{4.20}$$

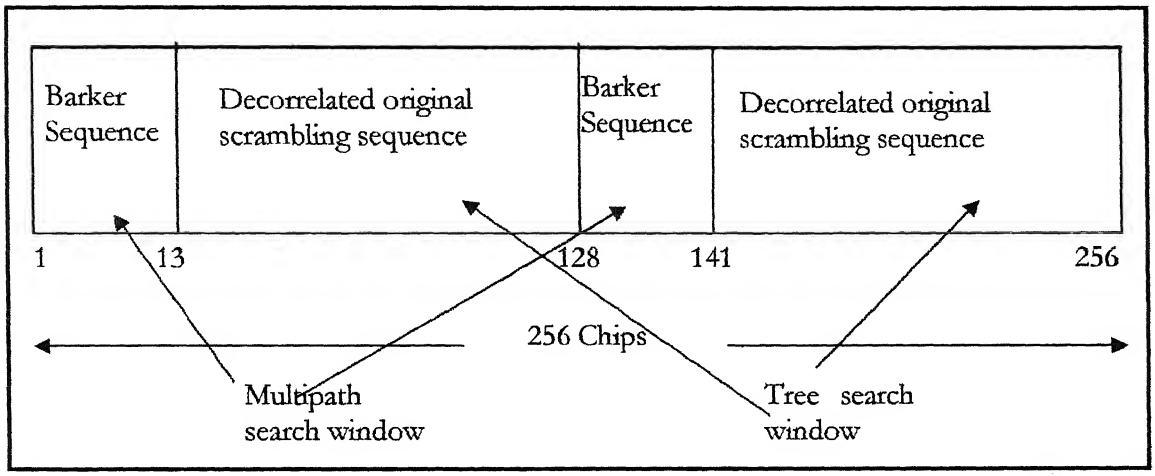

Figure 4.2: Decorrelated concatenated scrambling sequence

In (4.20), we have an interesting observation. The cross-correlation between the scrambling sequence and Barker sequence is reduced mainly to the correlation between Barker sequence and the decorrelator filter. This is shown in Figure 4.2. The maximum value of the correlation is unity when the relative delay between Barker sequence and decorrelator filter is zero and otherwise the value is either zero or 0.0769. In either of the conditions the value of $\rho_{lp}^{(k)}$ will depend on the summation of the original scrambling sequence over length 13. Due to the balance property of PN sequences, this summation will be a small value. When the signal at the output of the Barker CMF is passed through a square law detector, the value of this cross-correlation will be very small and merge with the background noise. Thus, this modified decorrelated and concatenated sequence will have a very low probability of false alarm rate.

In section 3.2 we have seen two separate cases of CFAR detection: first case is of a signal in Rayleigh fading channel and the second was for PN code acquisition. In the case of uplink

WCDMA, the CFAR detection scheme for multipath detection will be a combination of the two cases. After having reduced the correlation of out-of-phase signals to mere background noise, we can assume, without loss of generality that the detection scheme will be only of former kind and neglect the latter kind. The CFAR detection scheme followed will be that of Figure 3.4 where the governing equation is obtained from (3.18), (4.17) and (4.18)

$$\frac{1}{2}|Z_j|^2 > T\sum_{j=0}^{N_B-1}\frac{1}{2}|r(n-j)|^2$$

$$\frac{1}{2}|Z_j|^2 > \left((P_{FA})^{-1/N_B} - 1\right)\sum_{j=0}^{N_B-1}\frac{1}{2}|r(n-j)|^2 \qquad (4.21)$$

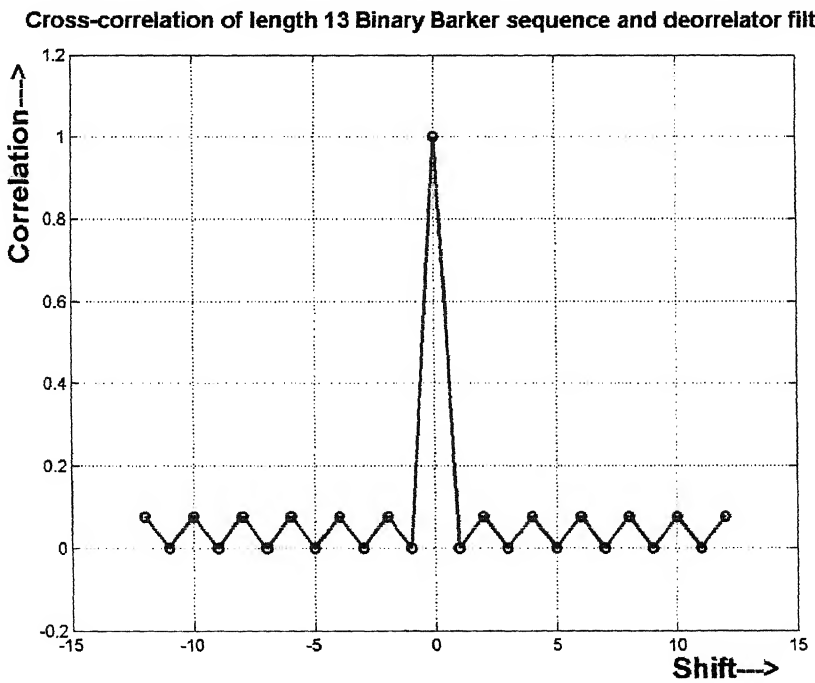

Figure 4.3: Cross-correlation of length 13 binary Barker sequence and decorrelator filter

Comment: The concatenated and de-correlated sequences have been obtained by modifying the existing scrambling sequences so as to enable detection of multipath signals in uplink WCDMA with low probability of false alarm. Since the original scrambling sequences

have been transformed/modified, their autocorrelation and cross-correlation properties should be studied and compared with that of the original sequences.

4.4 User Specific Code Acquisition

In (4.15) we have obtained a transformed sequence that will be used for code acquisition in our algorithm. After a multipath has been detected by (4.21), we commence user specific code acquisition within each multipath by Tree search using MHT. For this we use the scrambling sequence from the 14^{th} to 128^{th} chip. The code acquisition procedure will be carried out twice in one symbol duration of 256 chips. This will be done as:

- carryout multipath detection between 1^{st} and 13^{th} chip and 129^{th} and 141^{st} chips.
- once a multipath is detected at the end of 13^{th} chip, then carryout detection of users present in each multipath from the 14^{th} to 128^{th} chip.
- if a multipath is detected at the end of 141^{st} chip, then carryout detection of users present in each multipath from the 142^{nd} to 256^{th} chip.

The scrambling sequences prior to concatenation were binary and subsequent to concatenation and decorrelation are no longer binary. The consequence is that the codebook will become very complex and will be multi-valued. In the next section we will see how the sequences can be restored back to binary value at the BS.

4.4.1 Inverse Filtering

The WCDMA baseband signal processing is linear. The CMFs at the transmitter and the receiver can be designed using tapped delay line (TDL) filters. The weights of the Barker TDL filter and decorrelator are obtained by inverting the vectors given in (4.7) and (4.14). We shall use the same analogy in designing an Inverse Filter for reverting the decorrelated part of the

scrambling sequence to binary values. This will enable us to carryout tree search using a binary tree. The inverse filter to be designed should be inverse of the sequence in (4.14). Let us represent the Discrete Fourier transform of the vector in (4.14) by $D(k)$. Let the inverse of the transfer function be represented by $(D(k))^{-1}$. The two transfer function will be related as:

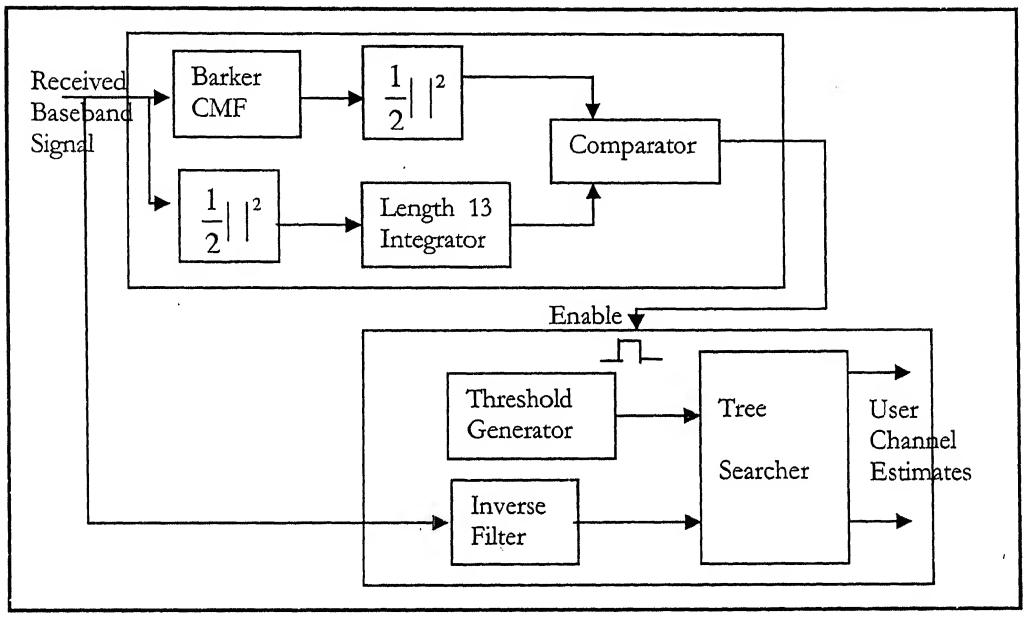

Figure 4.4: Proposed code acquisition algorithm

$$D(k)\left(D(k)\right)^{-1}=1$$
$$\left(D(k)\right)^{-1}=\frac{1}{D(k)} \tag{4.22}$$

The time domain representation of the inverse filter is given by:

$$\{d_n\}=F^{-1}\left(\left(D(k)\right)^{-1}\right)=\begin{pmatrix}0.86667,0.86667,-1.3,0.86667,-1.3,0.86667,0.86667,\\ -1.3,-1.3,0.86667,0.86667,0.86667,0.86667\end{pmatrix} \tag{4.23}$$

At the BS the chips arrive serially. The incoming chips are first passed through the CFAR detector. If a hit occurs indicating the existence of a multipath, the CFAR outputs a logical signal that enables a block that will carryout the tree search. The received baseband will pass

through the Inverse filter before being input to the tree searcher block as in Figure 4.4. This will restore the part of scrambling sequence back to the original signal corrupted by MAI, IPI and noise.

4.4.2 Partial Correlation of Scrambling Sequence

Tree search involves MHT wherein a hypothesis testing is done after each sample and the test is terminated when the test statistic crosses either the upper (selection) or lower (rejection) threshold. As against this, there is the conventional match filter approach of section 2.7.1 that does FSS test. For FSS type of tests, the test statistics will depend on the correlation of PN sequence over its entire length while MHT will depend on partial correlation. In this section we shall analyse the partial correlation of the original scrambling sequences.

In section 3.3.3 and 3.3.4 analysis of MHT is given. In this section we shall derive bounds for partial correlation only for the tree search part of the sequence and not the entire modified sequence. The partial correlation of a PN sequence is given by [51]:

$$R_w(k,l) = \sum_{i=1}^{w} \hat{c}_{i+k}^{(m)}\, \hat{c}_{i+l}^{(p)}, \qquad 0 \le k,l \le N-1 \tag{4.24}$$

which is a function of the initial phases k and l, the length of the correlation w and m and p are the two different user codes. If $m = p$, then it is autocorrelation else it gives cross-correlation. When $m = p$ and $k = l$, then H_1 is true and $R_w(k,l)$ is linear. When $k \neq l$, under H_0, then we have $R_w(k,l)$ in the worst case situation, which is approximated as linear. We obtain by simulation the approximate expressions for bounds on the mean and variance of $R_w(k,l)$.

$$E\{R_w(k,l)\} = \sum_{i=1}^{w} \overline{\hat{c}_{i+k}^{(m)}\, \hat{c}_{i+l}^{(p)}}$$

$$\cong \begin{cases} \frac{w}{N}, & \text{under } H_1 \\ \frac{0.5w}{N} & \text{under } H_0 \end{cases} \tag{4.25}$$

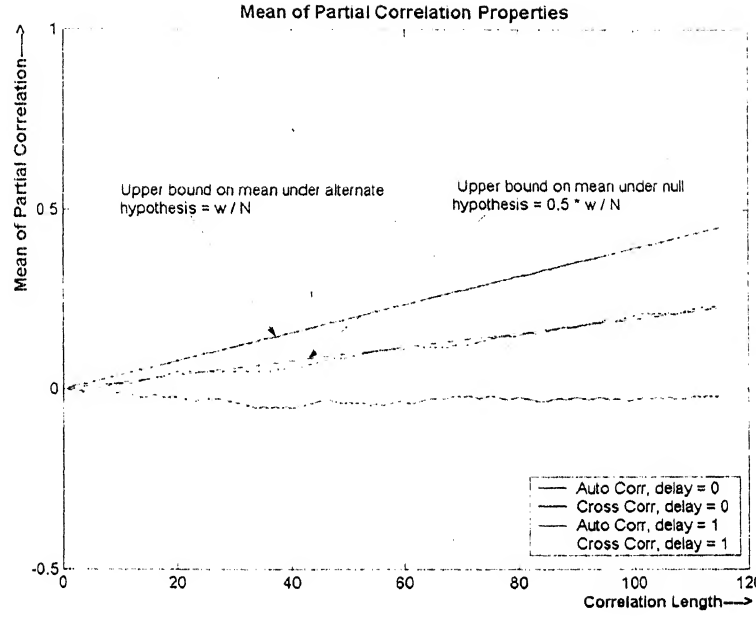

Figure 4.5: Mean of partial correlation of scrambling code

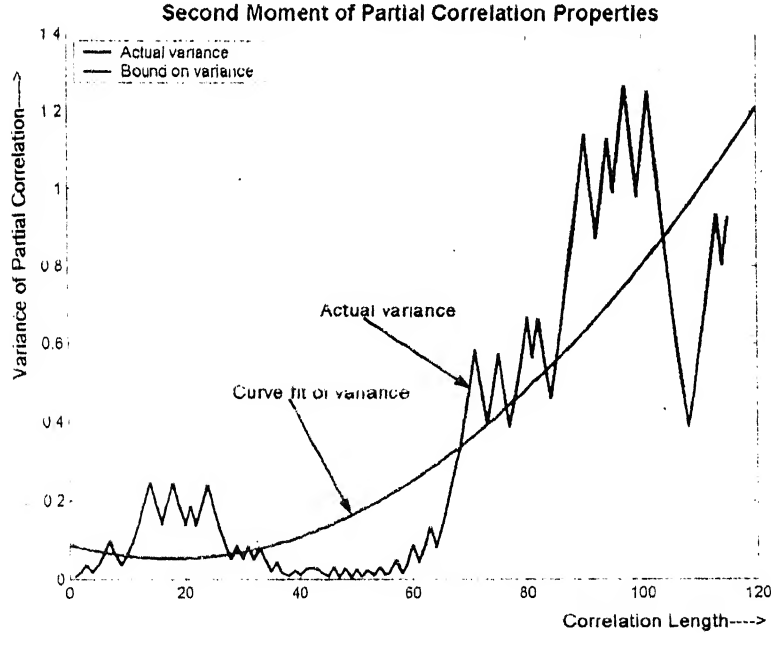

Figure 4.6: Variance of partial correlation of scrambling code

and $E\{R_w^2(k,l)\}=\sum_{i=1}^{w}\sum_{j=1}^{w}\overline{\hat{c}_{i+k}^{(m)}\,\hat{c}_{i+l}^{(p)}\,\hat{c}_{j+k}^{(m)}\,\hat{c}_{j+l}^{(p)}}$. The variance is given by

$$v^2 \equiv w\left(0.012741-\frac{0.0328w}{N}\right) \tag{4.26}$$

These values will be used for MHT variables θ_0, θ_1 and v^2 for designing the thresholds for tree detection.

4.4.3 Data Structure and Algorithm Description

In this stage of code acquisition we will use MHT as described earlier to prune the code tree. In case no users are detected in a multipath implies that it is a noise only path and a false alarm has been raised. Because multiple hypothesis are tested jointly, some users that are deemed to contain noise-only components will be eliminated simultaneously while others that are deemed to contain signal energy are detected simultaneously. The lower T-SPRT thresholds B, and upper thresholds A, and truncation stage threshold are designed using equations (3.61), (3.62) and (3.63) by setting the parameters as in (4.25) and (4.26).

Because we expect to complete code acquisition in one symbol period, the maximum number of stages in the MHT is less than the number of chips per symbol N, therefore we rewrite:

$$N_t = \min(\hat{N}_t, N) \tag{4.27}$$

where $\hat{N}_t$ is calculated by equation (3.53), (3.65) and (3.66). The following information is stored within each tree node:

- The current test stage i i.e., the tree depth level of node j.
- PN code value of tree node j.
- The test statistic of its father node where i is the tree depth level and j is the tree node identifier.

- A linked list that contains all paths that intersect this node.

The tree search part of code acquisition is a combination of tree search, code correlation and sequential detection. We denote, $Z_{i,j}$ as the T-SPRT test statistic of tree node (i, j), $r(i)$ as the i^{th} signal chip sample to be processed and $ZF_{i,j}$ is the input test statistic of the father node of tree node (i,j). The algorithm is executed as follows:

1. Initialise test statistic value at the tree root node (tree depth level 0) as $Z_{0,1} = 0$ and input this value to tree nodes (1,1), (1,2), i.e. $ZF_{1,1} = ZF_{1,2} = 0$.

2. Recursively execute the test in depth level i by breadth-first tree search. All the tree nodes at tree depth level i are tested. The test statistic value at tree node (i, j) is computed by:

$$Z_{i,j} = C_{i,j} * r(i) + ZF_{i,j} \tag{4.28}$$

   - If $Z_{i,j} \leq B_i$, the subtree from this tree node is discarded from further processing.
   - If $Z_{i,j} \geq A_i$, recorded the detected paths intersecting with this tree node.
   - If $A_i < Z_{i,j} < B_i$, output $Z_{i,j}$ to its child nodes at stage $i+1$ and proceed to the next tree depth level, i.e., set $i = i + 1$ and repeat.

3. If the final stage is reached, i.e., $i = N_t$, and if all the tree nodes in this stage are tested, then terminate the test.

4.4.4 Channel State Information

If the output of the CMF/correlator used for a full length search yields a hit then the expectation of the output of the correlator given in (2.10) under the condition $Z_{ij} \geq \tau$ gives:

$$E\{Z_{ij}\} = \frac{1}{G}\left(\beta_{ij} G + IN_{ij}\right)$$

$$= \beta_{ij} + \frac{IN_{ij}}{G}$$
$$\approx \beta_{ij} \tag{4.29}$$

The second term is negligible as compared to the first term in the event of a *hit* occurs. Therefore, expectation the output of the CMF/correlator yields the channel estimate. In the case of a sequential search, the correlation can be considered to be "an incremental chip-sized code match filtering". This means that the output of the CMF is checked at each time index and if it crosses the upper or lower threshold, a detection or rejection occurs. If it does not cross then the output is checked at the next time index. Hence, an expectation of the expression in (4.28) results in the same value as in (4.9) when the decision statistics is greater than the upper threshold. Given that $Z_{i,j} \geq A_i$ in (4.28) we have:

$$E\{Z_{i,j}\} = \frac{1}{i}\left(C_{i,j} * r(i) + ZF_{i,j}\right)$$
$$\approx \beta_{ip} \tag{4.30}$$

which is the channel estimate for the p^{th} path of the i^{th} user. Thus the output of the tree search averaged over the stage at which it detection gives the channel estimate.

Chapter 5

Performance of Code Acquisition Algorithm

5.1 Introduction

In the previous chapters we have developed the necessary theoretical background for the modified code acquisition scheme for WCDMA uplink. It is difficult to evaluate the performance of the sequential tests because their calculation rapidly becomes unmanageable even under certain simple conditions [52] [51]. For example, when the sequential test is used in a noncoherent receiver with a Gaussian noise channel, it is difficult to analyse due to the unavoidable modified Bessel function in the likelihood function [53] [51]. The problem is further compounded by the fact that very little literature is available for the study of uplink code acquisition under structured interference. Uplink code acquisition is rather complicated even under AWGN channel [9]. Thus, the only other alternative available for studying the performance is with the help of computer simulations.

5.2 Software Experiments

In order to get a realistic result for the uplink WCDMA code acquisition, we have designed the experiments as per the WCDMA specification TS 25 series [54]. We have taken a systems approach rather than a pure mathematical approach. The simulations have been carried out on Matlab 6.5 and Simulink 5.0.

5.2.1 Uplink Transmitter

The uplink transmitter design is as shown in Figure 5.1. The transmitter consists of a pilot sequence generator which consists of a trial of continuous ones at 15 Kbps. This is then spread by the scrambling code at the rate of 3.84 Mcps. The scrambling code type is different for

different experiments (as has been described in the previous chapter) and varies from user to user. The signal is next scaled by a factor β as has been shown in Figure 2.1. This baseband signal is then passed through a transmitter pulse shaping filter with a root-raised cosine (RRC) roll-of-factor of 0.22, oversample factor of 8, filter sampling frequency of 1/(3.84e-6) Hz and has 96 filter taps. After this the signal passes through the multipath channel. The multipath channel uses a fading profile with a maximum Doppler shift of 40 Hz (pedestrian case) [54] to fade the signals. Each user has two or three multipaths. As has been mentioned earlier, without loss of generality, we assume that timing adjustment and power control are existing in the system. Therefore, the users have the first path either with 0 or 1 chip delay, second multipath of 2 or 3 chip delay and third multipath of 4 chip delay. Thereafter, the signal passes through an AWGN channel which adds noise to the signal.

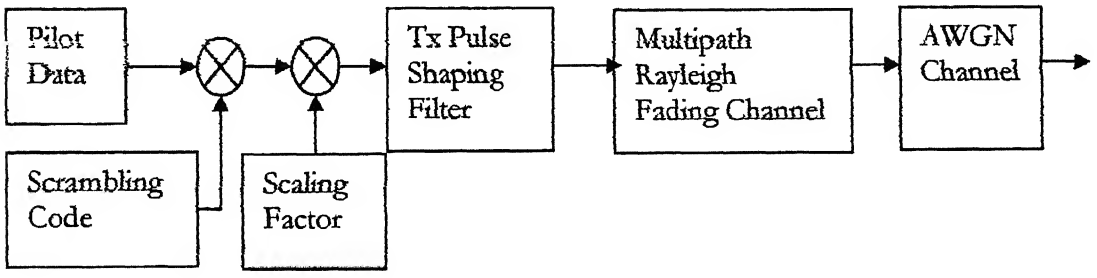

Figure 5.1: Uplink transmitter used in simulation

5.2.2 Uplink Receiver

The WCDMA uplink baseband receiver used for the simulation is as shown in Figure 5.2. The multipath faded and noise corrupted signal from different users is added at the receiver front end. The received signal is then passed through a receive pulse shaping filter with the same parameters as the transmitter pulse shaping filter. The upsampled signal is then downsampled to 3.84 Mcps. Thereafter, the receiver signal processing is as shown in Figure 4.4.

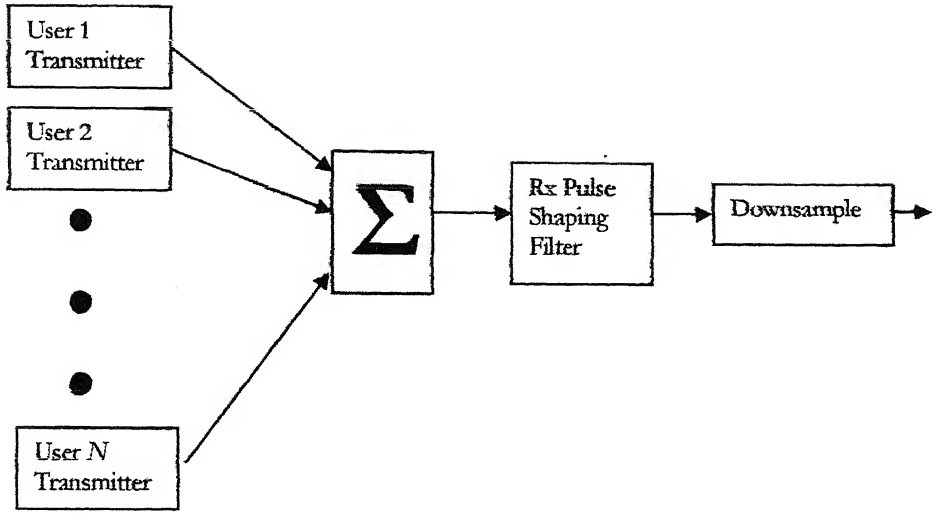

Figure 5.2: Uplink receiver baseband signal processing used in simulation

5.3 Performance of Modified Sequence

In section 4.3.2 we have analysed the concatenation of short scrambling codes that are described in section 2.2.2 with Barker sequence of length 13. In this section we will evaluate the consequence of this concatenation by simulation.

5.3.1 Concatenation by Barker Sequence

In order to resolve multipath signals at the BS, we have proposed concatenation of the scrambling sequence with Barker sequence. The sequence is as given in (4.10). A wilful correlation is introduced between the signals of different users to enable joint detection. For this part of the experiment we have a single user system with three multipaths under Rayleigh fading channel with path delays of T_c, $2T_c$ and $4T_c$, where T_c is the chip time and has relative mean power of -3dB, -6dB and -9dB. The output at the Barker CMF is given in Figure 5.3.

Comment: We observe that due to the cross-correlation between the 14^{th} – 128^{th} and 142^{nd} – 256^{th} chip and the Barker CMF results in false peaks. This is as given by (4.13). This will cause false alarms in the system. These false peaks need to be removed.

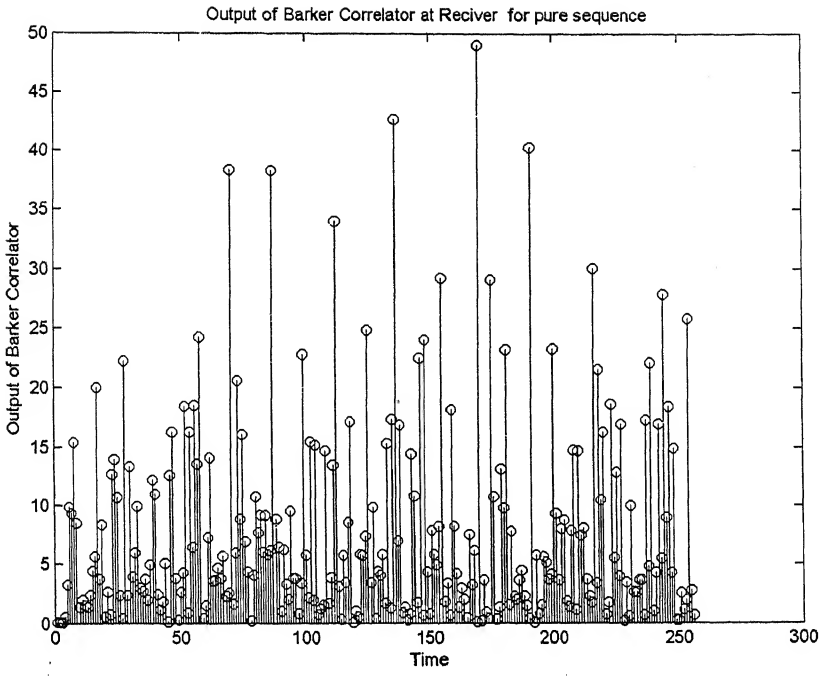

Figure 5.3: Cross-correlation of spreading sequence and Barker sequence

5.3.2 Performance of Decorrelated and Concatenated Sequence

We now investigate the sequence that has been obtained by further modification and given by (4.17). The scrambling code is modified by decorrelating the 14^{th} – 128^{th} and 142^{nd} – 256^{th} chip of the scrambling code. The simulation is carried out with same parameters as in section 5.3.1. The squared output at the Barker CMF is shown in Figure 5.4. The statistics of the simple concatenated sequence given by (4.8) and concatenated and decorrelated sequence of (4.15) at the output of Barker CMF is given in Table 5.1.

Comment: In the previous section we have noticed that the concatenated sequence gives a large number of false peaks. In Figure 5.4, we observe that as given in (4.20) the false peaks have been largely reduced resulting in lower false alarm rate. A comparison of the statistical properties of the two sequences substantiates the fact that decorrelated and concatenated sequence will perform better in CFAR detectors.

properties of the two sequences substantiates the fact that decorrelated and concatenated sequence will perform better in CFAR detectors.

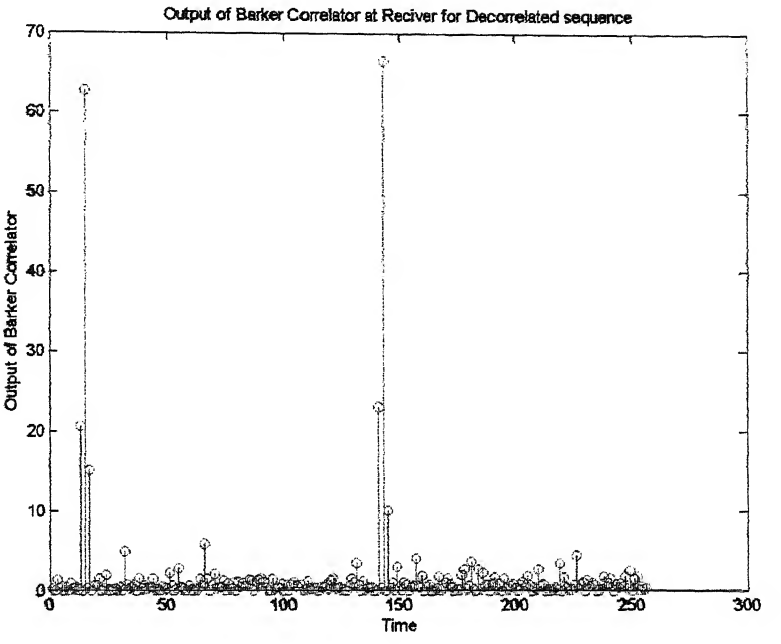

Figure 5.4: Cross-correlation of de-convolved spreading sequence and Barker sequence

Statistical Properties	Pure Sequence	Decorrelated Sequence
Mean value	12.1493	0.9307
Median	9	0.4793
Standard deviation	16.1744	1.4636

Table 5.1: Comparison of statistical properties of modified sequences.

5.3.3 Correlation Properties

In the previous section we have seen the benefits of decorrelated and concatenated sequences when it comes to CFAR detection at the output of a CMF matched to Barker sequence. The decorrelation so carried out over the short scrambling codes should be checked for any undesirable effects due to this transformation. The short scrambling code provides identity to each transmitter in the uplink and their correlation properties should be retained. Any

undesirable change in the correlation properties can cause interference to the other channels.

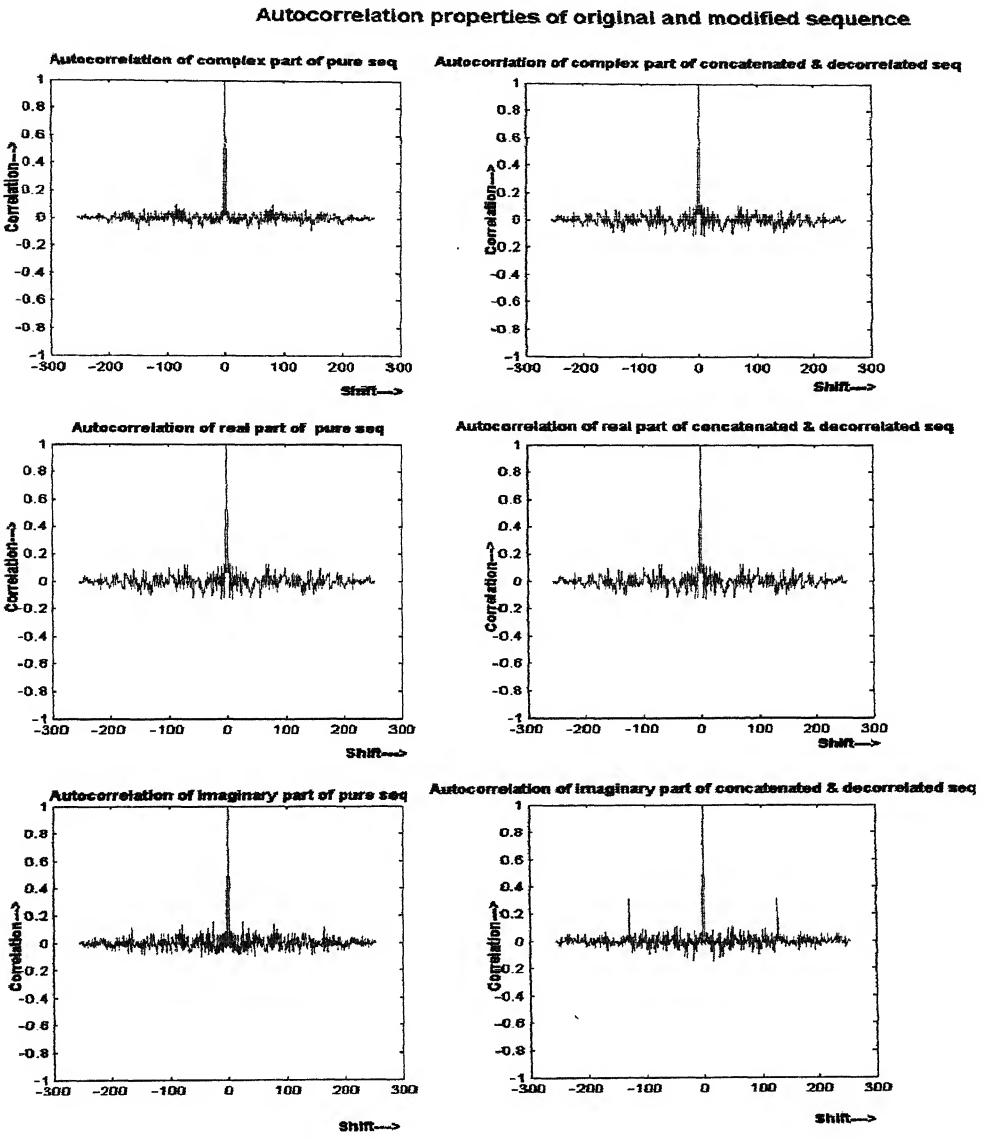

Figure 5.5: Autocorrelation properties of pure short spreading sequence and decorrelated concatenated sequence

We shall now see the complex, real and imaginary autocorrelation and cross-correlation properties of pure sequence (without decorrelation and concatenation) and the modified sequence.

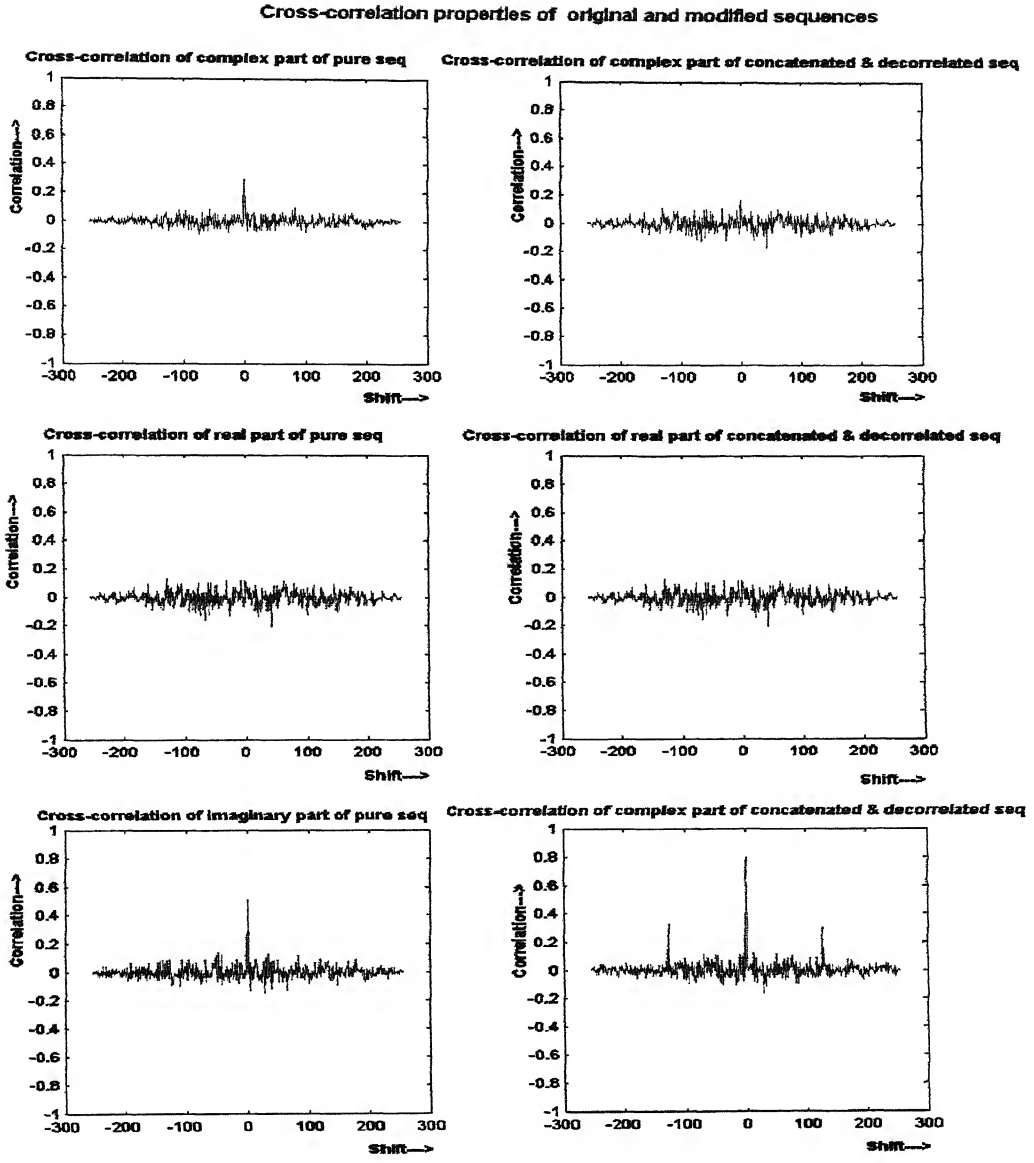

Figure 5.6: Cross-correlation properties of pure short spreading sequence and deconvolved concatenated sequence

In Figure 5.5 we observe that the autocorrelation properties of the pure and modified sequences are maintained except for the imaginary case (which has been modified). The two other short peaks are due to the Barker sequence and are not of much significance during tree search as this part of the sequence is not used in tree search. In Figure 5.6, we observe that there is an increase in the cross-correlation in the case of the imaginary parts due to the

presence of the same Barker code concatenation for all the sequences in the family. Under similar reasoning as above, we can ignore the marginal excess correlation.

5.3.4 Spectral Properties

Having seen the autocorrelation and cross-correlation properties of the pure and modified sequence we also see the spectral properties of the sequences. In Figure 5.7, we observe that

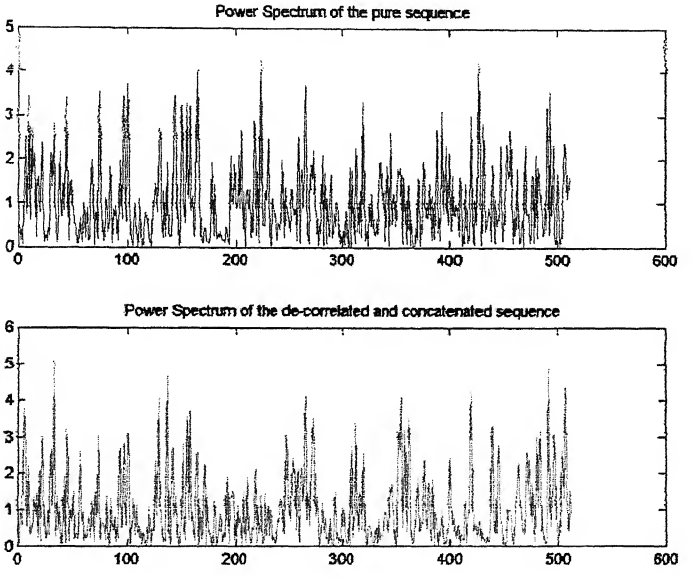

Figure 5.7: Comparison of spectral properties of pure and modified sequence.

Statistical Properties	Pure Sequence	Decorrelated Sequence
Maximum value	4.249	5.098
Mean value	1	1
Median	0.8214	0.6563
Standard deviation	0.8623	0.9799
Range	4.249	5.098

Table 5.2: Comparison of statistical properties of power spectrum

the spectrum is noise like in both the cases. The statistical properties of the power spectrum show very little changes. We, therefore, conclude that the properties of the modified sequence do not vary much and the added benefit is that we get better performance of multipath detection using Barker sequence.

5.4 Multipath Detection Performance using CFAR

In this section we will analyse the performance of the CFAR detection system. First we analyse the system for a single user case with varying SNR and false alarm (threshold for CFAR) and then we study its performance for multiuser case under Rayleigh fading. The former test is a rather deterministic test to ascertain performance of the receiver design. The latter test is for the actual WCDMA code acquisition.

5.4.1 CFAR Detector in AWGN Channel: Single User

We have seen the properties of the decorrelated and concatenated sequence in the previous section. The probability of miss detection for various false alarm rates is simulated for different

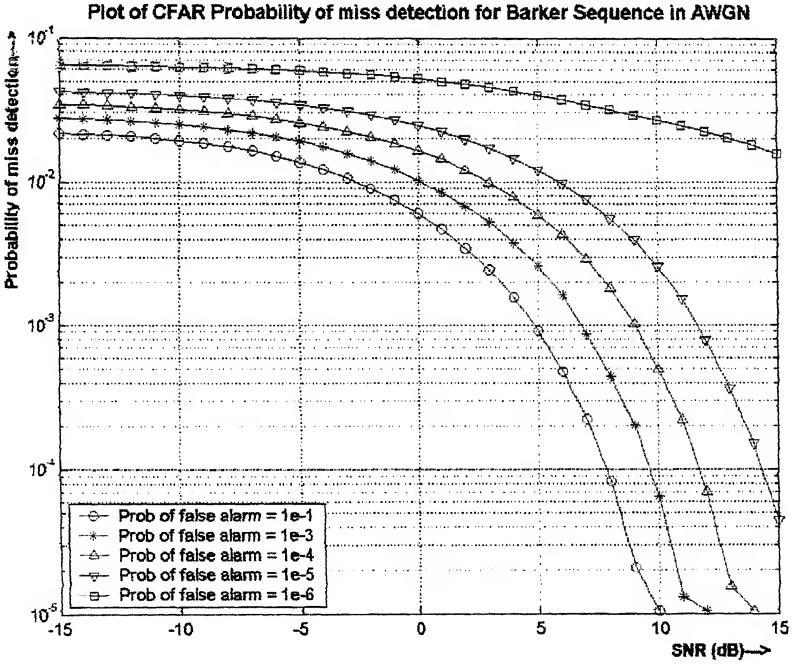

Figure 5.8: Probability of miss detection versus SNR for different false alarm

values of SNR in an AWGN channel. The threshold for the different false alarm rate is given by (3.18). Using this value as the threshold for the CFAR detection, we first study the performance of the detector in an AWGN channel for a single user case. The probability of

detection is given by (3.16). The results of simulation for probability of detection versus SNR for different values of false alarm are given in Figure 5.8. The plots in the figures indicate that with increase in SNR, the probability of miss detection decreases and the probability of detection increases. For lower values of false alarm rate, there is lower probability of detection as more path detections are missed owing to higher threshold value for detection.

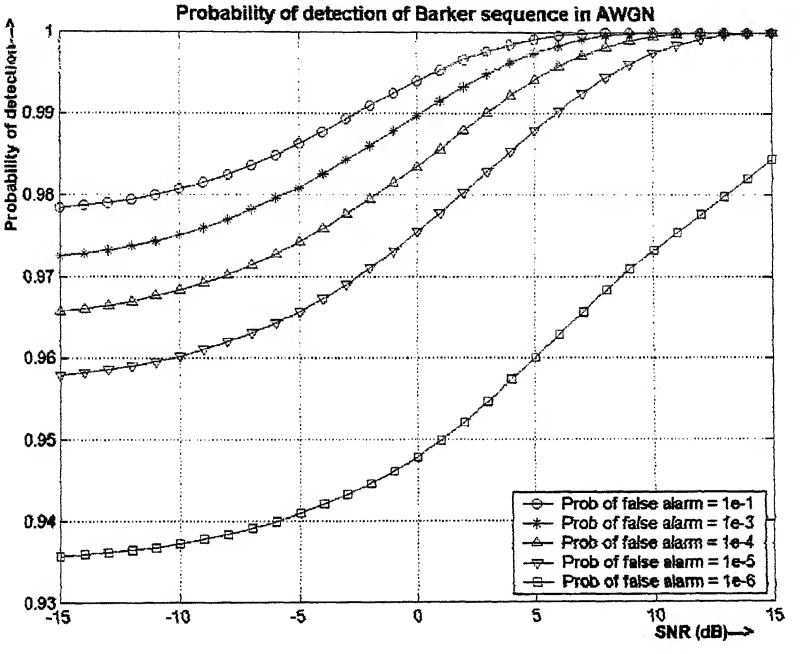

Figure 5.9: Probability of detection versus SNR for different false alarm

5.4.2 CFAR Detection of Multipath Rayleigh Fading: Multiuser

In the multiuser case, we simulate the probability of miss detection and probability of false alarm in a Rayleigh fading channel. There are three paths in the uplink. In this simulation we have assumed timing alignment [1] for all users which are under the power control of the base station. This essentially means that the first path of all users has zero or one chip-time relative delay. No inter-cell interference is considered. Power control is assumed and hence near-far

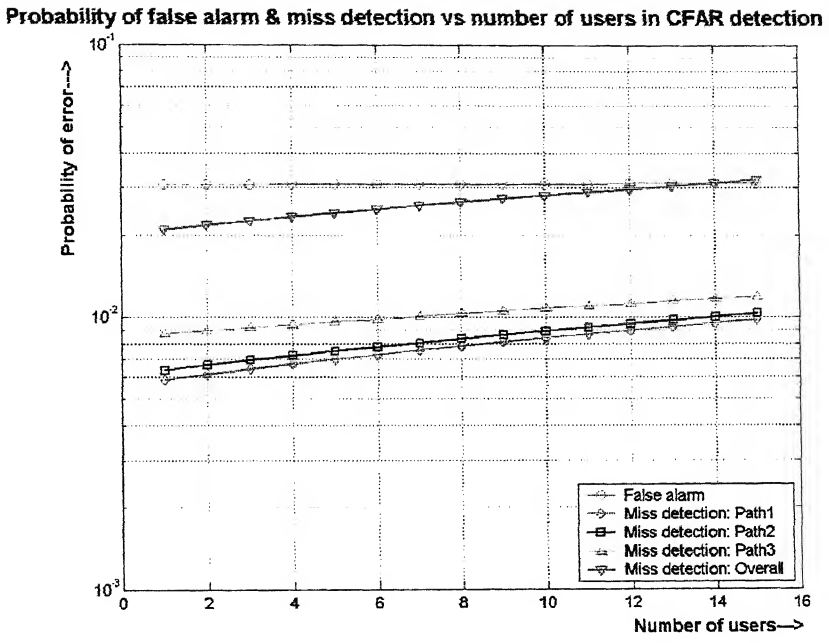

Figure 5.10: Probability of false alarm and miss detection versus the number of users in CFAR detection.

effect due to cell-geometry is neglected. The assumptions are valid since the searcher carries out code-acquisition for traffic channels. A MS can send traffic only when other synchronization as required in cell-search procedure has been achieved. Figure 5.10 shows the probability of miss detection for all the three paths and the total miss detection of the system. The simulation is carried out for 15 users. We observe that the probability of miss detection approaches a limit after a certain number of users become active in a system. This is due to the correlation of the Barker sequence part of the scrambling code. The output of the Barker CMF should be above the specified threshold and once this level is achieved, subsequent increase in signal power due to increased number of users having the same relative delay, does not change the probability of miss detection. In Figure 5.10 we observe that the false alarm rate is constant and is the same as that of the design parameter.

5.5 Performance of Code Acquisition by Tree Search

In this section we analyse the performance of the tree search detection system which is used for user specific code acquisition. The signals arriving at the BS are Rayleigh faded and the

correlation of the scrambling codes due to larger number of users is considered Gaussian as per Central Limit Theorem [45].

5.5.1 Inverse Filter

The scrambling code is modified at the transmitter by decorrelating the 14^{th} – 128^{th} and 142^{nd} – 256^{th} chip of the scrambling code with a decorrelator filter in order to reduce the false alarm in CFAR detector. The sequence will have to be restored back to its original form for tree search detection. This is achieved with the help of inverse filtering and defined in (4.23). In order to analyze the performance of the inverse filter, we shall compare the received waveform at the BS of the sequence defined by (4.8) and (4.15). The former sequence

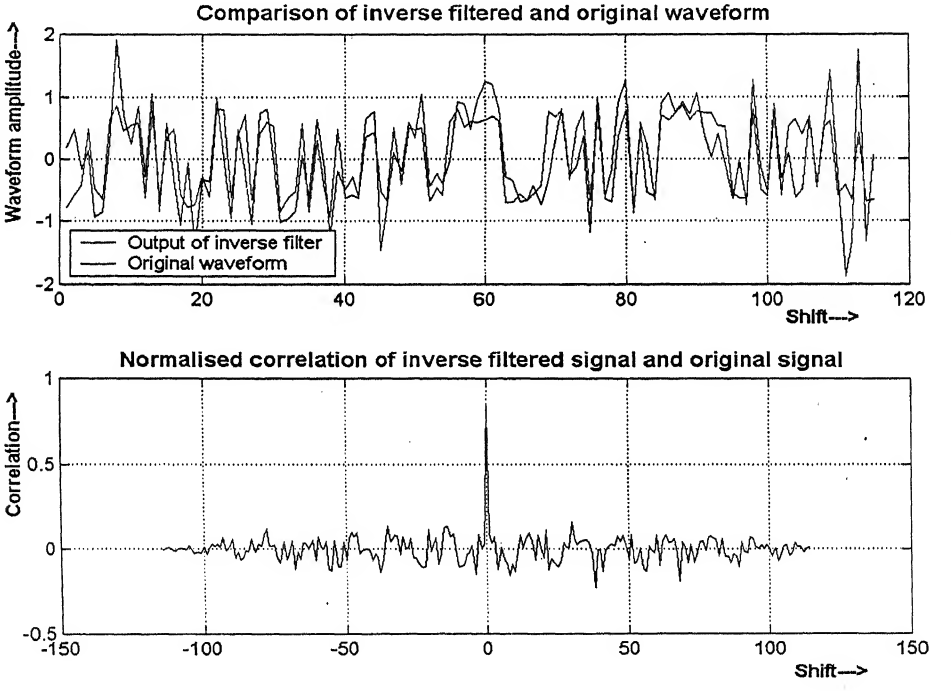

Figure 5.11: Comparison of inverse filter output signal with original sequence

is without decorrelation and the latter sequence is with decorrelation and inverse filtered. The two sequences are obtained at the end of a multipath Rayleigh faded channel corrupted by AWGN. We also correlate the output of the inverse filter with the original sequence. We find

AWGN. We also correlate the output of the inverse filter with the original sequence. We find that the output of the inverse signal is highly correlated with the original sequence. The inverse filter restores back the decorrelated part of the scrambling sequence.

5.5.2 Performance of MHT

The output of the CFAR detector is used to enable a tree search block. The CFAR block also provides the value of γ which is the scaling factor for the threshold for MHT. In the present simulation, we have considered multipath Rayleigh fading channel in the presence of Gaussian noise. The users have either two or three multipath with the first path either with 0 or 1 chip delay, second multipath of 2 or 3 chip delays or third multipath of 4 chip delays. The design parameters chosen are $P_f = 0.05$, $P_M = 0.1$ and $c_1 = c_2 = 0.5$. We have used the parameters obtained from the partial correlation bounds obtained in section 4.4.2. The plots for probability of miss detection for different multipaths for the number of active users in the system are shown in Figure 5.12. In Figure 5.13, we have the probability of false alarm for each of the multipath shown against variation of users in the system.

Comments: The value of the joint channel estimate obtained from the CFAR system is used to dynamically change the upper and lower threshold for the MHT. We have the following observations:

- The relative mean power of the first path is -3 dB, the second path is -6 dB and the third path is -9 dB. We compare the equations for the thresholds in (3.61), (3.62) and (3.63) with that of the equation of a straight line $y = mx + c$, where m is the slope and c is the intercept. We find that the intercept is divided by the factor γ. For stronger paths the intercept will be small since γ is higher for stronger paths. The two thresholds will be closer and steeper. This causes some of the test statistics to cross the upper

threshold resulting in false alarm. Thus the first path has a moderate miss detection probability.

- The third path has a converse approach than the first path. When there are fewer users in the system, the value of γ is low and the thresholds are wider apart. Due to interference from stronger path signal, the test statistics cross the upper threshold. This results in the path having least probability of miss detection. With the addition of more users in the system, the value of γ becomes higher resulting in steeper and narrower thresholds. This prevents the test statistics from crossing the upper threshold. Instead they clear the lower threshold and have higher probability of miss detection. This also results in lesser false alarm.
- In comparison to the first and the last delay paths, the second path shows a mixed performance. The dynamic thresholds hold good for most conditions and it approaches the design probabilities of false alarm and miss detection.

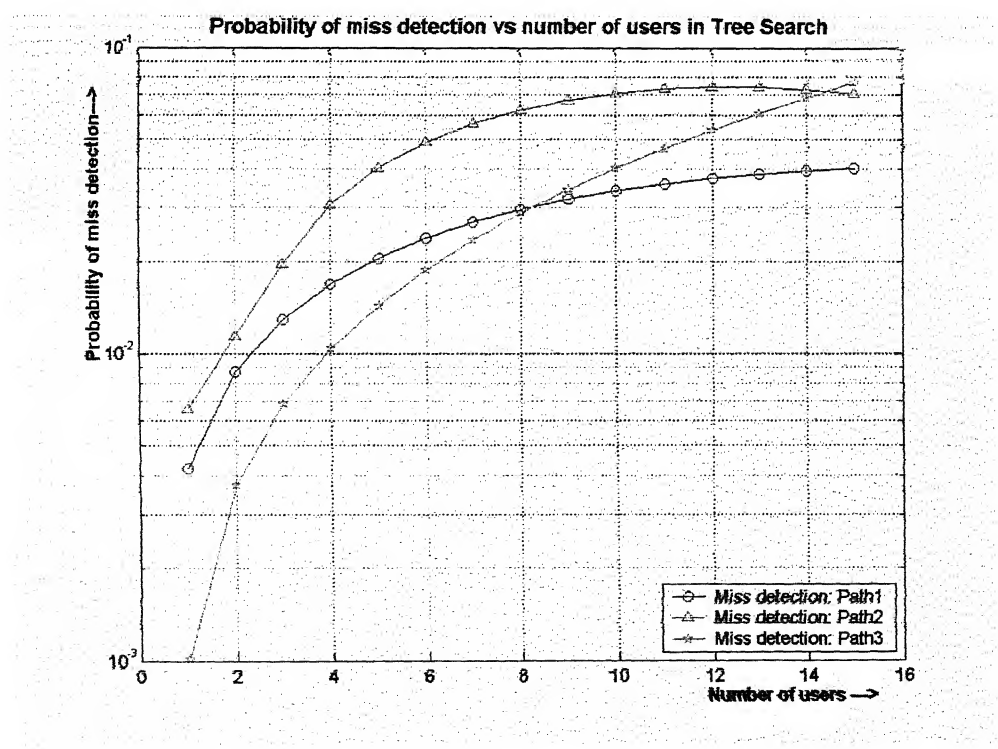

Figure 5.12: Plot of Probability of miss detection versus number of users in tree search

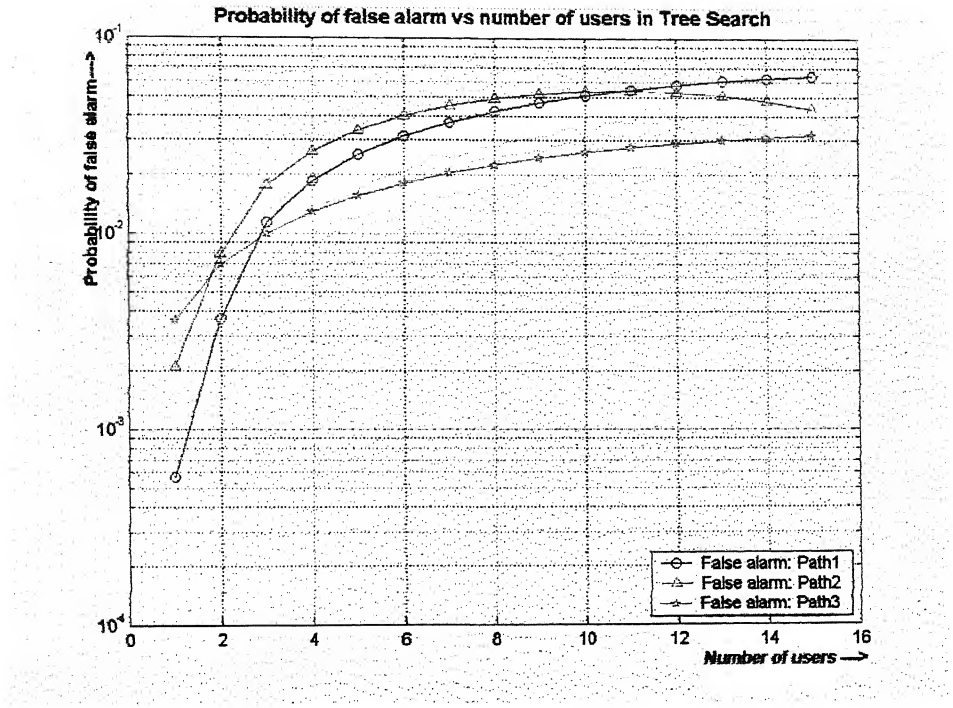

Figure 5.13: Plot of Probability of false alarm versus number of users in tree search

5.5.3 Average Sample Number

The average sample number is the number of samples required by the TSPRT to make a decision. This factor depends on the values of c_1 and c_2. We have chosen the values to be such that the test is an equal mixture of FSS and SPRT. The plot is shown in Figure 5.14.

Comments: The plot shows that when there are fewer users in the system, for paths with higher relative mean power, the threshold being higher requires more number of samples while it is the other way round for weaker paths. As the interference rises, the weaker path requires more samples to make a decision and the stronger paths require lesser number of samples. This is commensurate with the results in Figure 5.14. Thus the number of samples required using TSPRT is much lesser than that of a full search and the code acquisition is fast.

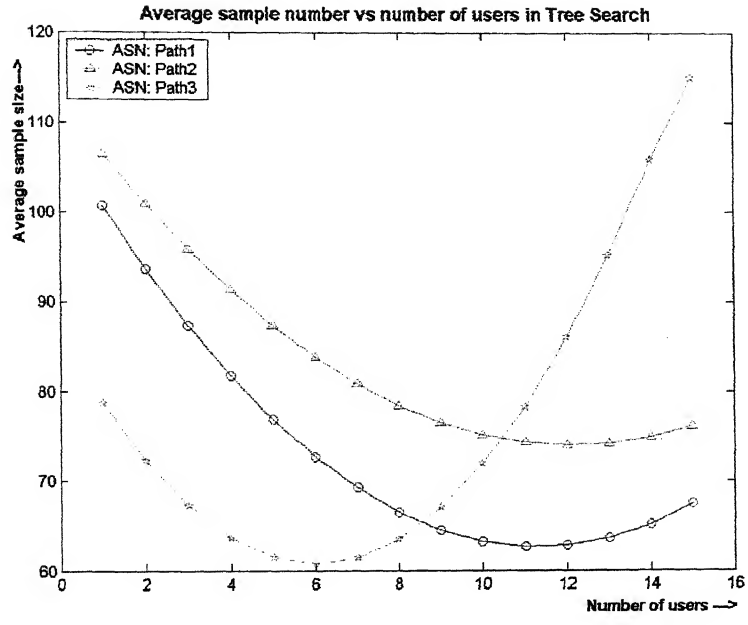

Figure 5.14: Average number of samples required for detection

Conclusions

In this chapter we have seen that by concatenating the existing scrambling sequence with Barker sequence, we are able to detect the existing multipaths at the BS in 13 chips duration. By decorrelating the scrambling sequence between 14^{th} – 128^{th} and 142^{nd} – 256^{th} chip with the inverse of Barker sequence we are able to contain the false alarm rate to the designed parameter. User specific code acquisition is achieved by tree search using MHT. The sequential test has reduced computational complexity and it requires lesser number of samples as compared to FSS. Therefore the acquisition is faster. If the test prolongs to the truncation stage as would be the case for weaker paths, then the total acquisition time required is 128 chips. But for the stronger paths the acquisition is achieved in lesser number of samples. However, the price paid is that the probability of false alarm and miss detection are higher.

Chapter 6

Conclusions and Future Work

This chapter summarizes the major contributions in this thesis and presents possible future directions which could be extension of the research work in this thesis.

6.1 Conclusion

It had been proved by Abraham Wald that sequential tests need much less sample size than a FSS test. Thus, systems employing sequential tests have a lower computational complexity than FSS tests. TSPRT requires much lesser sample size than a FSS for the same probabilities of false alarm and miss detection. We have proposed a new algorithm using the excellent autocorrelation properties of the Barker sequence along with tree search detection for the code acquisition problem.

The probability of false alarm for multipath detection can be a chosen design parameter. For the tree search using MHT, the error probabilities obtained are less than or equal to that of the design parameters. The average sample size is for decision is much lower than the FSS test sample size.

6.2 Future Work

- For the CFAR detection system we have analysed the statistical model for a Rayleigh fading channel. Similar analysis needs to be done for Rician fading and log-normal shadowing channels.

- For MHT we have analysed under Gaussian channel conditions and for Rayleigh faded signals at the output of a CMF. It is suggested that sequential CFAR detection be employed for tree search [55].

- The thresholds for TSPRT have been modified from the threshold derived for Gaussian distribution. It will be worthwhile to derive these for other distribution using asymptotic analysis.

- The theoretical analysis for the acquisition time using TSPRT for paths with varying SNR can be made as given in [56] [51].

- The existing system can be extended to multiple antenna systems using 2-D Rake receiver.

Bibliography

[1] H. Holma and A. Toskala, *WCDMA based for UMTS: Radio Access for Third Generation Mobile Communications*: John Wiley.

[2] E. Dahlman, B. Gudmundson, M. Nilsson, and J. Skold, "UMTS/IMT-2000 based on wideband CDMA," *IEEE Communications Magazine*, pp. 70-80, 1998.

[3] F. Adachi and M. Sawahashi, "Wideband wireless access based on DS-CDMA," *IEICE Transactions on Communications*, vol. E81-B, pp. 1305-1316, 1998.

[4] F. Adachi, M. Sawahashi, and H. Suda, "Wideband DS-CDMA for next generation mobile communications systems," *IEEE Communications Magazine*, pp. 56-69, 1998.

[5] R. Peterson, R. Ziemer, and D. Borth, *Introduction to Spread Spectrum Communications*: Prentice Hall, 1995.

[6] J. Proakis, *Digital Communication*, 3 ed. Toronto: Mcgraw-Hill, 1995.

[7] T. Rapparport, *Wireless Communications - Principles and Practices*. Toronto: Prentice Hall, 1996.

[8] J. Liberti and R. TS, *Smart antennas for wireless communications: IS-95 and Third Generation CDMA Applications*: Prentice Hall, 1999.

[9] A. Viterbi, *CDMA: Principles of Spread Spectrum Communications*: Addison-Wesley, 1995.

[10] R. Rick and L. Milstein, "Parallel acquisition in mobile DS-CDMA systems," *IEICE Transactions on Communications*, vol. 45, pp. 1466-1476, 1997.

[11] B. Dong and S. Blostein, "Low complexity PN code acquisition with search wideband CDMA multipath channels.," presented at ICC '03, 2003.

[12] U. Cheng, "Performance of a class of parallel spread spectrum acquisition scheme in the presence of data modulation," *IEEE Transactions on Communications*, vol. 38, pp. 596-604, 1998.

[13] C. Deng, "A Burst Mode PN acquisition processor for Direct Sequence Spread Spectrum." Los Angeles: University of California, 1998. http://www.janet.ucla.edu/glomo/finalreport/final_report_documents/cdeng_ms-thesis.pdf

[14] H. Chang, Y. Park, and Y. Lee, "DS-SS acquisition based on simultaneous search and verification," presented at IEEE Vehicular Technology Conference, 1998.

[15] L. Wei, "Near optimum tree search detection schemes for bit-synchronous multiuser CDMA systems over Gaussian and two-path Rayleigh-fading channels," *IEEE Transactions on Communications*, vol. 45, pp. 691-700, 1997.

[16] Z. Xie, C. Rushforth, R. Short, and T. Moon, "Joint signal detection and parameter estimation in multiuser communications," *IEEE Transactions on Communications*, vol. 41, pp. 1208-1215, 1997.

[17] A. Bhargave, R. Figneiredo, and T. Eltoft, "A detection algorithm for the V-BLAST system," presented at Global Telecommunication Conference, 2001.

[18] G. Stuber, *Principle of Mobile Communication*: Kulwer Academy, 1996.

[19] W. Lee, "Overview of cellular CDMA," *IEEE Transactions on Vehicular Technology*, vol. 40, pp. 299-302, 1991.

[20] R. Pickholtz, I. Milstein, and D. Schilling, "Spread spectrum for mobile communication," *IEEE Transactions on Vehicular Technology*, vol. 40, pp. 313-322, 1991.

[21] K. Gilhousen, I. Jacobs, R. Padovani, A. Viterbi, L. Weaver, and C. Wheatly, "On capacity of a cellular CDMA systems," *IEEE Transactions on Vehicular Technology*, vol. 40, pp. 303-312, 1991.

[22] W. Braun, "PN acquisition and tracking performance in DS/CDMA systems with symbol length spreading sequences," *IEICE Transactions on Communications*, vol. 45, pp. 1595-1601, 1997.

[23] F. Dinan and B. Jabbari, "Spreading codes for direct sequence CDMA and wideband CDMA cellular networks," *IEEE Communications Magazine*, pp. 48-55, 1998.

[24] L. Milstein, "Wideband code division multiple access," *IEEE Transactions on Selected Areas in Communication*, vol. 18, pp. 1344-1354, 2000.

[25] H. Andoh, M. Sawahashi, and F. Adachi, "Channel estimation using time-multiplexed pilot symbol for coherent RAKE combining for DS-CDMA mobile radio," *IEICE Transactions on Communications*, vol. E81-B, pp. 1365-1373, 1998.

[26] N. T. Tin, "An experimental system for characterising wideband CDMA vector channels and smart antennas," Queen's University, 2000. http://ipcl.ee.queensu.ca/PAPERS/thesis_tinn.ps

[27] G. T.-R. W. Group, "Spreading and Modulation (FDD), Release 5," 3GPP TS 25.213 v 5.3.0 (online), 2003. http://www.3gpp.org/ftp/Specs/html-info/25213.htm

[28] S. Abeta, M. Sawahashi, and F. Adachi, "Performance comparison between time-multiplexed pilot channel and parallel pilot channel for coherent RAKE combining in

DS-CDMA mobile radio," *IEICE Transactions on Communications*, vol. E81-B, pp. 1417-1425, 1998.

[29] Y. Honda and K. Jamal, "Channel estimation based on time multiplexed pilot symbols," IEICE Technical Report RCS-96-70, August 1996.

[30] M. Mohar and J. Lodge, "TCMP - a modulation and coding strategy for Rician fading channel," *IEEE Transactions on Selected Areas in Communication*, vol. SAC - 7, pp. 1347-1355, 1989.

[31] J. Cavers, "An analysis of pilot symbol assisted modulation for Rayleigh fading channels," *IEEE Transactions on Selected Areas in Communication*, vol. VT - 40, pp. 689-693, 1991.

[32] S. Sampei and T. Sunaga, "Rayleigh fading compensation for QAM in land mobile radio communication," *IEEE Transactions on Vehicular Technology*, vol. VT - 42, pp. 137-147, 1993.

[33] M. Win, G. Chrisikos, and N. Solleberger, "Performance of RAKE reception in dense multipath channel: implication of spreading bandwidth and selection diversity order," *IEEE Transactions on Selected Areas in Communication*, vol. 18, pp. 1516-1525, 2000.

[34] Y. Lee and S. Kim, "Sequence acquisition of DS-CDMA systems employing Gold Sequences," *IEEE Transactions on Vehicular Technology*, vol. 495, pp. 2397-2407, 2000.

[35] S. Fukumolo, M. Sawahashi, and F. Adachi, "Matched filter - based RAKE combiner for wideband DS-CDMA mobile radio," *IEICE Transactions on Communications*, vol. E81-B, pp. 1384-1391, 1998.

[36] I. Garvanov, "Methods and algorithms for keeping false alarm rate in the presence of pulse jamming." BAS, Bulgaria: Institute of Information Technologies, 2003. http://www.iit.bas.bg/staff_en/i_garvanov2.html

[37] J. DIFranco and W. Rubin, *Radar Detection.* USA: Artech House, 1980.

[38] B. Farina, "Netting and Signal Processing Strech Radar Surveillance," *AFCEA*, vol. Signal, pp. 73-81, 1991.

[39] P. Swerling, "More on detection of Fluctuating Targets (Corresp)," *IEEE Transactions on Information Theory*, vol. 11, pp. 459-460, 1965.

[40] P. Swerling, "Probability of detection for fluctuating targets," *IEEE Transactions on Information Theory*, vol. 6, pp. 269-308, 1960.

[41] V. Behar, C. Kabakchiev, and L. Doukovaska, "Adaptive CFAR PI Processor for Radar Target Detection in Pulse Jamming," *Journal of VLSI Signal Processing*, vol. SP-26, pp. 383-396, 2000.

[42] T. Namekawa, X. Hou, and N. Morinaga, "Direct evaluation of Radar detection proabilities," *IEEE Transactions on Aerospace and Electronic Systems*, vol. AES - 23, pp. 418-423, 1987.

[43] P. Gandhi and S. Kassam, "Analysis of CFAR Processor in homogenous background," *IEEE Transactions on Aerospace and Electronic Systems*, vol. AES-24, pp. 427-445, 1988.

[44] K. R. Griep, J. J. Burlingame, and J. Ritcey, "CFAR acquisition of DS-SS codes for CDMA ranging," presented at Twenty-Eighth Conference on Signals, Systems and Computers, Asilmora, 1994.

[45] K. S. Shanmugam and A. Breipohl, *Random Signals Detection, Estimation and Data Analysis.* New York: John Wiley & Sons, 1988.

[46] H. V. Poor, *An introduction to signal detection and estimating.* New York: Springer-Verlag, 1994.

[47] S. Blostein and T. Huang, "Detection of small moving objects in image sequences using sequential hypothesis testing," *IEEE Transactions on Signal Processing*, vol. SP-39, pp. 1611-1629, 1991.

[48] S. Tantaratana and H. Poor, "Asymptotic efficiencies of truncated sequential tests," *IEEE Transactions on Information Theory*, vol. IT-28 no 6, pp. 911-923, 1982.

[49] A. Wald, *Sequential Analysis.* New York: Wiley, 1947.

[50] S. Golomb and R. Scholtz, "Generalised Barker sequences," *IEEE Transactions on Information Theory*, vol. 11, pp. 533-537, 1965.

[51] Y.-H. Lee and S. Tantaratana, "Sequential Acquisition of PN Sequences for DS/SS Communications: Design and Performance," *IEEE Selected Areas in Communications*, vol. 10, pp. 750-759, 1992.

[52] D. Siegmund, *Sequential Analysis.* New York: Springer-Verlag, 1985.

[53] J. Bussgang and D. Middleton, "Optimum sequential detection of signals in noise," *IEEE Transactions on Information Theory*, pp. 5-18, 1955.

[54] 3GPP, "3GPP Specification series," R6 ed: 3GPP, 2004. http://www.3gpp.org/ftp/Specs/html-info/25-series.htm

[55] 3GPP, "TS 25.133 v6.6.0 Requirements for support of radio resource management," 3GPP, Valbonne - France June 2004. http://www.3gpp.org/ftp/Specs/html-info/25133.htm

[56] T. S, "Sequential CFAR detectors using a Dead-Zone Limiter," *IEEE Transactions on Communications*, vol. 38, pp. 1375-1383, 1990.

[57] O.-S. Shin and K. B. E. Lee, "Utilization of multipaths for spread-spectrum code acquisition in frequencey-selective Rayleigh fading channels," *IEEE Transactions on Communications*, vol. 49, pp. 734-743, 2001.